Available online at www.sciencedirect.com
ScienceDirect
Comput. Methods Appl. Mech. Engrg. 196 (2007) 1244–1260
Computer methods in applied mechanics and engineering
www.elsevier.com/locate/cma

On the stability of the reduced basis method for Stokes equations in parametrized domains

Gianluigi Rozza [a,*], Karen Veroy [b]

[a] CMCS – Modeling and Scientific Computing, EPFL – Ecole Polytechnique Fédérale de Lausanne, Station 8, CH1015 Lausanne, Switzerland
[b] Mechanical Engineering Department, MIT – Massachusetts Institute of Technology, 77 Mass Avenue, Room 3-264, Cambridge, MA 02139, USA

Received 30 March 2006; received in revised form 6 September 2006; accepted 7 September 2006

Abstract

We present an application of reduced basis method for Stokes equations in domains with affine parametric dependence. The essential components of the method are (i) the rapid convergence of global reduced basis approximations – Galerkin projection onto a space W_N spanned by solutions of the governing partial differential equation at N selected points in parameter space; (ii) the off-line/on-line computational procedures decoupling the generation and projection stages of the approximation process.

The operation count for the on-line stage – in which, given a new parameter value, we calculate an output of interest – depends only on N (typically very small) and the parametric complexity of the problem; the method is thus ideally suited for the repeated and rapid evaluations required in the context of parameter estimation, design, optimization, and real-time control. Particular attention is given (i) to the pressure treatment of incompressible Stokes problem; (ii) to find an equivalent inf–sup condition that guarantees stability of reduced basis solutions by enriching the reduced basis velocity approximation space with the solutions of a supremizer problem; (iii) to provide algebraic stability of the problem by reducing the condition number of reduced basis matrices using an orthonormalization procedure applied to basis functions; (iv) to reduce computational costs in order to allow real-time solution of parametrized problem.

Keywords: Parametrized Stokes equations; Reduced basis methods; Approximation stability; Inf–sup condition; Supremizer; Galerkin approximation; Algebraic stability; Gram–Schmidt basis orthogonalization

1. Introduction

The optimization, control, design and characterization of an engineering component or system requires the prediction of certain "quantities of interest," or performance metrics, which we denote *outputs* – for example velocity field, maximum stresses, maximum temperatures, heat transfer, flow rates, vorticity, or lifts and drags. These outputs are typically expressed as functionals of field variables associated with parametrized partial differential equations (P^2DE) which describe the physical behavior of the system. The parameters, which we shall denote *inputs*, serve to identify a particular "configuration" of the components: these inputs may represent design or decision variables, such as geometry, or characterization variables, such as physical properties – for example in inverse design problems. We thus get an implicit *input–output* relationship whose evaluation demands the solution of the underlying partial differential equations.

The development of computational methods is permitting *rapid* and *reliable* evaluation of this input–output relationship in the design, optimization and control contexts. The approach used is based on the reduced basis method, first introduced in the late 1970s for nonlinear structural analysis, and later developed more broadly in the 1980s and 1990s (see [1,3] for general framework, [24] for extension to multi-parameter problems, [4,16] for application in nonlinear problems). Recent applications of the method

* Corresponding author. Tel.: +41 21 6932733; fax: +41 21 6934303.
E-mail addresses: gianluigi.rozza@epfl.ch (G. Rozza), veroy@alum.mit.edu (K. Veroy).

0045-7825/$ - see front matter
doi:10.1016/j.cma.2006.09.005

are contained in [14,18–20,25,33]. For the general a priori convergence properties of reduced basis method see, for example, [11,12].

In the application we use *global* approximation spaces and we exploit *off-line/on-line* computational decompositions (see [1] for application of this strategy within the reduced basis context). These steps allow us – for the class of "parameter-affine" problems – to reliably decouple the generation and projection stages of reduced basis approximation, thereby effecting computational economies of several orders of magnitude.

In this paper we deal with the application and investigation of reduced basis techniques for Stokes equations in parametrized domains, focusing our attention to pressure treatment, to approximation stability (by the introduction of an equivalent inf–sup condition) and to algebraic stability (by achieving condition number reduction and basis orthonormalization). Preliminary applications of reduced basis techniques to incompressible viscous flow problems are given in [15,10] and also [9] for optimal control problems; however in these contributions the pressure approximation is not considered and stability of solutions is not discussed. More recent works dealing with divergence-free velocity spaces, physical parameters and focused on a posteriori error estimates are the ones by Patera et al. [31,14,32]. After this introduction, in Section 2 we formulate the problem for parametrized Stokes equations. In Section 3 we introduce the Stokes reduced basis formulation and analyze the stability of the approximation. At the end of this section we introduce an application of the method to a "T-bypass" configuration. In Section 4 we study a procedure to control N more tightly and to apply an adaptive procedure for the basis construction using a suitable error projection. In Section 5 we analyze the inf–sup condition which is necessary for the stability of reduced basis approximation. Then in Section 6 we present some numerical results for three different test cases based on the same geometrical configuration. In Section 7 we deal with algebraic stability problem and we present possible solutions to achieve it by orthonormalization. In Section 8 we mention possible developments for viscous flow and shape optimization problem in haemodynamics within the reduced basis framework.

2. The parametrized Stokes problem

We consider the following steady Stokes problem [5] in a domain $\widehat{\Omega} \subset \mathbb{R}^2$ with boundary $\widehat{\Gamma}$:

$$\begin{cases} -\nu\triangle\tilde{\mathbf{u}} + \nabla\hat{p} = \hat{\mathbf{f}} \quad \text{in } \widehat{\Omega}, \\ \nabla\cdot\tilde{\mathbf{u}} = 0 \quad \text{in } \widehat{\Omega}, \\ \tilde{\mathbf{u}} = \mathbf{0} \quad \text{on } \widehat{\Gamma}_{\mathrm{w}}; \qquad \tilde{\mathbf{u}} = \hat{\mathbf{g}}_{\mathrm{in}} \quad \text{on } \widehat{\Gamma}_{\mathrm{in}}; \\ \nu\dfrac{\partial\tilde{\mathbf{u}}}{\partial\hat{\mathbf{n}}} - \hat{p}\hat{\mathbf{n}} = \mathbf{0} \quad \text{on } \widehat{\Gamma}_{\mathrm{out}}, \end{cases} \tag{1}$$

where $\tilde{\mathbf{u}}$ is the velocity, $\hat{p}$ the pressure, $\hat{\mathbf{f}}$ a force field, ν a kinematic viscosity and $\hat{\mathbf{n}}$ is the normal unit vector. The boundary $\partial\widehat{\Omega}$ is split into three components, $\widehat{\Gamma}_{\mathrm{w}}, \widehat{\Gamma}_{\mathrm{in}}, \widehat{\Gamma}_{\mathrm{out}}$, such that the Dirichlet portion $\widehat{\Gamma}_D = \widehat{\Gamma}_{\mathrm{w}} \cup \widehat{\Gamma}_{\mathrm{in}}$. After introducing a lift function $\hat{L}_{\hat{\mathbf{g}}_{\mathrm{in}}}$ (extension of non-homogeneous boundary conditions to the interior of the domain) such that $\hat{\mathbf{u}} = \tilde{\mathbf{u}} - \hat{L}_{\hat{\mathbf{g}}_{\mathrm{in}}}$ and $\hat{\mathbf{u}}|_{\Gamma_D} = 0$, the weak formulation of (1) reads: find $\hat{\mathbf{u}} \in \widehat{Y} = H^1_{\widehat{\Gamma}_D}(\widehat{\Omega}) \times H^1_{\widehat{\Gamma}_D}(\widehat{\Omega})$, (where $H^1_{\widehat{\Gamma}_D}(\widehat{\Omega}) = \{u \in H^1(\widehat{\Omega}) : u = 0 \text{ on } \widehat{\Gamma}_D\}$), $\hat{p} \in \widehat{M} = L^2(\widehat{\Omega})$ such that

$$\begin{cases} \nu\displaystyle\int_{\hat{\Omega}} \nabla\hat{\mathbf{u}} \otimes \nabla\hat{\mathbf{w}}\,\mathrm{d}\Omega - \int_{\hat{\Omega}} \hat{p}\nabla\cdot\hat{\mathbf{w}}\,\mathrm{d}\Omega \\ \qquad = \displaystyle\int_{\hat{\Omega}} \hat{\mathbf{f}}\cdot\hat{\mathbf{w}}\,\mathrm{d}\Omega + \langle\widehat{F}^0, \hat{\mathbf{w}}\rangle, \quad \forall\hat{\mathbf{w}} \in \widehat{Y}, \\ \displaystyle\int_{\hat{\Omega}} \hat{q}\nabla\cdot\hat{\mathbf{u}}\,\mathrm{d}\Omega = \langle\widehat{G}^0, \hat{q}\rangle, \quad \forall\hat{q} \in \widehat{M}, \end{cases} \tag{2}$$

$\widehat{F}^0, \widehat{G}^0$ are terms due to non-homogeneous Dirichlet boundary condition ($\tilde{\mathbf{u}} = \hat{\mathbf{g}}_{\mathrm{in}}$) on $\widehat{\Gamma}_{\mathrm{in}}$, on $\widehat{\Gamma}_{\mathrm{out}}$ we have a stress-free Neumann condition. We assume that the domain is made up of R sub-domains: $\widehat{\Omega} = \bigcup_{r=1}^{R} \widehat{\Omega}^r$, so that the bilinear and linear forms of the weak formulation read for $1 \leqslant i, j \leqslant 2$ and $\hat{\nu}_{i,j} = \nu\delta_{i,j}$ as

$$\langle\widehat{\mathscr{A}}\hat{\mathbf{u}}, \hat{\mathbf{w}}\rangle = \sum_{r=1}^{R} \int_{\hat{\Omega}^r} \hat{\nu}_{ij} \frac{\partial\hat{\mathbf{u}}}{\partial\hat{x}_i} \cdot \frac{\partial\hat{\mathbf{w}}}{\partial\hat{x}_j}\,\mathrm{d}\widehat{\Omega}, \tag{3}$$

where summation over i and j is understood,

$$\langle\widehat{\mathscr{B}}\hat{p}, \hat{\mathbf{w}}\rangle = -\sum_{r=1}^{R} \int_{\hat{\Omega}^r} \hat{p}\nabla\cdot\hat{\mathbf{w}}\,\mathrm{d}\widehat{\Omega}, \tag{4}$$

$$\langle\widehat{F}, \hat{\mathbf{w}}\rangle = \langle\widehat{F}_s, \hat{\mathbf{w}}\rangle + \langle\widehat{F}^0, \hat{\mathbf{w}}\rangle \tag{5}$$

and

$$\begin{aligned} \langle\widehat{F}_s, \hat{\mathbf{w}}\rangle &= \sum_{r=1}^{R} \int_{\hat{\Omega}^r} \hat{f}\hat{\mathbf{w}}\,\mathrm{d}\widehat{\Omega}, \langle\widehat{F}^0, \hat{\mathbf{w}}\rangle \\ &= -\langle\widehat{\mathscr{A}}\hat{L}_{\hat{\mathbf{g}}_{\mathrm{in}}}, \hat{\mathbf{w}}\rangle, \\ \langle\widehat{G}^0, \hat{q}\rangle &= \langle\widehat{\mathscr{B}}\hat{q}, \hat{L}_{\hat{\mathbf{g}}_{\mathrm{in}}}\rangle. \end{aligned} \tag{6}$$

Then we write

$$\begin{cases} \langle\widehat{\mathscr{A}}\hat{\mathbf{u}}, \hat{\mathbf{w}}\rangle + \langle\widehat{\mathscr{B}}\hat{p}, \hat{\mathbf{w}}\rangle = \langle\widehat{F}, \hat{\mathbf{w}}\rangle, \quad \forall\hat{\mathbf{w}} \in \widehat{Y}, \\ \langle\widehat{\mathscr{B}}\hat{q}, \hat{\mathbf{u}}\rangle = \langle\widehat{G}^0, \hat{q}\rangle, \quad \forall\hat{q} \in \widehat{M}. \end{cases} \tag{7}$$

We want to build a system of parametrized partial differential equations (P^{2}DEs) depending on a set of geometrical parameters $\boldsymbol{\mu} = \{\mu_1, \ldots, \mu_P\} \in \mathscr{D}^{\mu} \subset \mathbb{R}^P$, that we call parameters. Then (7) is traced back to a *reference domain* by an *affine mapping* of the sub-domains $\widehat{\Omega}^r$ into Ω^r. For any $\hat{\mathbf{x}} \in \widehat{\Omega}^r$, $r = 1, \ldots, R$, its image $\mathbf{x} \in \Omega^r$ is given by

$$\mathbf{x} = \mathscr{G}^r(\boldsymbol{\mu};\ \hat{\mathbf{x}}) = G^r(\boldsymbol{\mu})\hat{\mathbf{x}} + g^r, \quad 1 \leqslant r \leqslant R; \tag{8}$$

we thus write

$$\frac{\partial}{\partial\hat{x}_i} = \frac{\partial x_j}{\partial\hat{x}_i}\frac{\partial}{\partial x_j} = G^r_{ji}(\boldsymbol{\mu})\frac{\partial}{\partial x_j} \tag{9}$$

and we get in the reference domain Ω:

$$\langle \mathscr{A}\mathbf{u},\mathbf{w}\rangle = \sum_{r=1}^{R}\int_{\Omega^r}\frac{\partial \mathbf{u}}{\partial x_i}\left(G^r_{ii'}(\boldsymbol{\mu})\hat{v}_{i'j'}G^r_{jj'}(\boldsymbol{\mu})\det(G^r(\boldsymbol{\mu}))^{-1}\right)\frac{\partial \mathbf{w}}{\partial x_j}\,\mathrm{d}\Omega,\quad \forall \mathbf{w}\in Y, \tag{10}$$

$$\langle \mathscr{B}p,\mathbf{w}\rangle = -\sum_{r=1}^{R}\int_{\Omega^r} p\left(G^r_{ij}(\boldsymbol{\mu})\det(G^r(\boldsymbol{\mu}))^{-1}\right)\frac{\partial w_j}{\partial x_i}\,\mathrm{d}\Omega,\quad \forall \mathbf{w}\in Y, \tag{11}$$

$$\langle F,\mathbf{w}\rangle = \langle F_s,\mathbf{w}\rangle + \langle F^0,\mathbf{w}\rangle, \tag{12}$$

where

$$\langle F_s,\mathbf{w}\rangle = \sum_{r=1}^{R}\int_{\Omega^r}\left(\hat{f}^r\det(G^r(\boldsymbol{\mu}))^{-1}\right)\mathbf{w}\,\mathrm{d}\Omega;\qquad \langle F^0,\mathbf{w}\rangle = -\langle \mathscr{A}\hat{L}_{\hat{\mathbf{g}}_{\mathrm{in}}},\mathbf{w}\rangle;\quad \langle G^0,q\rangle = \langle \mathscr{B}q,\hat{L}_{\hat{\mathbf{g}}_{\mathrm{in}}}\rangle. \tag{13}$$

The *transformation tensors* for the bilinear viscous terms are defined as follows:

$$v^r_{ij}(\boldsymbol{\mu}) = G^r_{ii'}(\boldsymbol{\mu})\hat{v}_{i'j'}G^r_{jj'}(\boldsymbol{\mu})\det(G^r(\boldsymbol{\mu}))^{-1},\quad 1\leqslant i,i',j,j'\leqslant 2,\ \ r=1,\ldots,R. \tag{14}$$

The tensors for *pressure and divergence forms* are

$$\chi^r_{ij}(\boldsymbol{\mu}) = G^r_{ij}\det(G^r(\boldsymbol{\mu}))^{-1},\quad 1\leqslant i,j\leqslant 2,\ \ r=1,\ldots,R. \tag{15}$$

Furthermore, we may define

$$\Theta^{q(i,j,r)}(\boldsymbol{\mu}) = v^r_{ij}(\boldsymbol{\mu}),\quad \langle \mathscr{A}^{q(i,j,r)}\mathbf{u},\mathbf{w}\rangle = \int_{\Omega^r}\frac{\partial \mathbf{u}}{\partial x_i}\cdot\frac{\partial \mathbf{w}}{\partial x_j}\,\mathrm{d}\Omega, \tag{16}$$

$$\Phi^{s(i,j,r)}(\boldsymbol{\mu}) = \chi^r_{ij}(\boldsymbol{\mu}),\quad \langle \mathscr{B}^{s(i,j,r)}p,\mathbf{w}\rangle = -\int_{\Omega^r} p\frac{\partial w_i}{\partial x_j}\,\mathrm{d}\Omega \tag{17}$$

for $1\leqslant r\leqslant R$, $1\leqslant i,j\leqslant 2$ (q and s are condensed indexes of i, j, r quantities) and we apply affine decomposition:

$$\mathscr{A}(\boldsymbol{\mu};\mathbf{u},\mathbf{w}) = \sum_{q=1}^{Q^a}\Theta^q(\boldsymbol{\mu})\mathscr{A}(\mathbf{u},\mathbf{w})^q; \tag{18}$$

$$\mathscr{B}(\boldsymbol{\mu};p,\mathbf{w}) = \sum_{s=1}^{Q^b}\Phi^s(\boldsymbol{\mu})\mathscr{B}(p,\mathbf{w})^s \tag{19}$$

for $\Omega\subset\mathbb{R}^{d=2}$, Q^a may be as large as $d\times d\times d\times R$ and Q^b as large as $d\times d\times R$.

This splitting of the operators into a part which is parameter-dependent and into a part parameter-independent (defined and computed once in the reference domain) is crucial for the computational efficiency of the method.

The Stokes problem rewritten on the reference domain Ω reads: find $(\mathbf{u}(\boldsymbol{\mu}),p(\boldsymbol{\mu}))\in Y\times M$ such that

$$\begin{cases}\mathscr{A}(\boldsymbol{\mu};\mathbf{u}(\boldsymbol{\mu}),\mathbf{w}) + \mathscr{B}(\boldsymbol{\mu};p(\boldsymbol{\mu}),\mathbf{w}) = \langle F,\mathbf{w}\rangle, & \forall \mathbf{w}\in Y,\\ \mathscr{B}(\boldsymbol{\mu};q,\mathbf{u}(\boldsymbol{\mu})) = \langle G^0,q\rangle, & \forall q\in M.\end{cases} \tag{20}$$

In our numerical approximation the Stokes problem has been solved by the Galerkin-Finite Element Method, see [6–8]. With the subscript h we indicate discretized quantities and finite dimensional sub-spaces like $V_h\subset V$ and $M_h\subset M$ for velocity ($\mathbf{u}_h$) and pressure (p_h), respectively. A necessary condition for the well posedness of this problem is the so-called *inf–sup condition* (LBB) [23]:

$$\exists\beta_0>0:\quad \beta(\boldsymbol{\mu}) = \inf_{q\in M_h}\sup_{\mathbf{w}\in Y_h}\frac{\mathscr{B}(\boldsymbol{\mu};q,\mathbf{w})}{\|\mathbf{w}\|_Y\|q\|_M}\geqslant\beta_0,\quad \forall\boldsymbol{\mu}\in\mathscr{D}^{\boldsymbol{\mu}}. \tag{21}$$

To verify it let us introduce a supremizer operator $T^{\boldsymbol{\mu}}$: $M_h\to Y_h$ defined as follows:

$$(T^{\boldsymbol{\mu}}q,\mathbf{w})_Y = \mathscr{B}(\boldsymbol{\mu};q,\mathbf{w}),\quad \forall\mathbf{w}\in Y_h; \tag{22}$$

so that

$$T^{\boldsymbol{\mu}}q = \arg\sup_{\mathbf{w}\in Y_h}\frac{\mathscr{B}(\boldsymbol{\mu};q,\mathbf{w})}{\|\mathbf{w}\|_Y}. \tag{23}$$

It is possible to demonstrate that

$$\beta^2(\boldsymbol{\mu}) = \inf_{q\in M_h}\frac{(T^{\boldsymbol{\mu}}q,T^{\boldsymbol{\mu}}q)_Y}{\|q\|^2_M}, \tag{24}$$

by definition (22) it follows that

$$\|T^{\boldsymbol{\mu}}q\|^2_Y = \mathscr{B}(\boldsymbol{\mu};q,T^{\boldsymbol{\mu}}q),$$

and by applying (23) and (21) we have

$$\inf_{q\in M_h}\frac{(T^{\boldsymbol{\mu}}q,T^{\boldsymbol{\mu}}q)_Y}{\|q\|^2_M} = \inf_{q\in M_h}\frac{\|T^{\boldsymbol{\mu}}q\|^2_Y}{\|q\|^2_M} = \inf_{q\in M_h}\left[\sup_{\mathbf{w}\in Y_h}\frac{(T^{\boldsymbol{\mu}}q,\mathbf{w})_Y}{\|\mathbf{w}\|_Y\|q\|_M}\right]^2 = \inf_{q\in M_h}\left[\sup_{\mathbf{w}\in Y_h}\frac{\mathscr{B}(\boldsymbol{\mu},q,\mathbf{w})}{\|\mathbf{w}\|_Y\|q\|_M}\right]^2 = \beta^2(\boldsymbol{\mu}),$$

this proves (24).

3. The reduced basis formulation of the Stokes equations

In the reduced basis approximation we take some "$\boldsymbol{\mu}$" samples $S^{\boldsymbol{\mu}}_N = \{\boldsymbol{\mu}^1,\ldots,\boldsymbol{\mu}^N\}$, where $\boldsymbol{\mu}^n\in\mathscr{D}^{\boldsymbol{\mu}}$, $n=1,\ldots,N$ and we solve N times the Stokes problem (20) using the Galerkin-Finite Element Method to obtain $\mathbf{u}_h(\boldsymbol{\mu})$ and $p_h(\boldsymbol{\mu})$.

The *reduced basis pressure space* is $M_N = \mathrm{span}\{\xi_n, n=1,\ldots,N\}$, where $\xi_n = p_h(\boldsymbol{\mu}^n)$.

We can build the *reduced basis velocity space* as $Y^{\boldsymbol{\mu}}_N = \mathrm{span}\{\zeta_n,\ n=1,\ldots,N;\ T^{\boldsymbol{\mu}}\xi_n,\ n=1,\ldots,N\}$, where $\zeta_n = \mathbf{u}_h(\boldsymbol{\mu}^n)$. The reduced basis approximation problem reads: find $(\mathbf{u}_N(\boldsymbol{\mu}),p_N(\boldsymbol{\mu}))\in Y^{\boldsymbol{\mu}}_N\times M_N$ such that

$$\begin{cases}\mathscr{A}(\boldsymbol{\mu};\mathbf{u}_N(\boldsymbol{\mu}),\mathbf{w}) + \mathscr{B}(\boldsymbol{\mu};p_N(\boldsymbol{\mu}),\mathbf{w}) = \langle F,\mathbf{w}\rangle, & \forall\mathbf{w}\in Y^{\boldsymbol{\mu}}_N,\\ \mathscr{B}(\boldsymbol{\mu};q,\mathbf{u}_N(\boldsymbol{\mu})) = \langle G,q\rangle, & \forall q\in M_N.\end{cases} \tag{25}$$

Problem (25) is subject to an equivalent reduced basis inf–sup condition.

Lemma 3.1. *We define*

$$\beta_N(\boldsymbol{\mu}) = \inf_{q\in M_N}\sup_{\mathbf{w}\in Y^{\boldsymbol{\mu}}_N}\frac{\mathscr{B}(\boldsymbol{\mu},q,\mathbf{w})}{\|\mathbf{w}\|_Y\|q\|_M}.$$

Then the following inequalities hold

$$\beta_N(\boldsymbol{\mu}) \geqslant \beta(\boldsymbol{\mu}) \geqslant \beta_0 > 0, \quad \forall \boldsymbol{\mu} \in \mathscr{D}^{\boldsymbol{\mu}}.$$

Proof

$$\begin{aligned}\beta(\boldsymbol{\mu}) &= \inf_{q\in M_h} \sup_{\mathbf{w}\in Y_h} \frac{\mathscr{B}(\boldsymbol{\mu},q,\mathbf{w})}{\|\mathbf{w}\|_Y\|q\|_M} \leqslant \inf_{q\in M_N} \sup_{\mathbf{w}\in Y_h} \frac{\mathscr{B}(\boldsymbol{\mu},q,\mathbf{w})}{\|\mathbf{w}\|_Y\|q\|_M} \\ &= \inf_{q\in M_N} \frac{\mathscr{B}(\boldsymbol{\mu};q,T^{\boldsymbol{\mu}}q)}{\|T^{\boldsymbol{\mu}}q\|_Y\|q\|_M} \leqslant \inf_{q\in M_N} \sup_{\mathbf{w}\in Y_N^{\boldsymbol{\mu}}} \frac{\mathscr{B}(\boldsymbol{\mu},q,\mathbf{w})}{\|\mathbf{w}\|_Y\|q\|_M} \\ &= \beta_N(\boldsymbol{\mu}). \qquad \square\end{aligned}$$

To demonstrate the lemma above we have applied the fact that $M_N \subset M_h$, the definition of the supremizer and the fact that the velocity space is enriched by supremizers, respectively. For further considerations on supremizer operator and the reduced basis framework, see [25] for the general non-coercive problem and [34] especially for Helmholtz and Burgers equations.

We rewrite for computational convenience $Y_N^{\boldsymbol{\mu}}$ using the *affine dependence* of $\mathscr{B}(\boldsymbol{\mu},q,\mathbf{w})$ on the parameter and the *linearity* of $T^{\boldsymbol{\mu}}$: $T^{\boldsymbol{\mu}}\xi = \sum_{q=1}^{Q^b} \Phi^q(\boldsymbol{\mu}) T^q \xi$ for any ξ and $\boldsymbol{\mu}$, which allows us to write

$$Y_N^{\boldsymbol{\mu}} = \operatorname{span}\left\{ \sum_{k=1}^{\overline{Q}^b} \Phi^k(\boldsymbol{\mu})\boldsymbol{\sigma}_{kn}, \quad n = 1,\ldots,2N \right\},$$

where $\overline{Q}^b = Q^b + 1, \Phi^{\overline{Q}^b} = 1$.
For $n = 1,\ldots,N$:

$$\boldsymbol{\sigma}_{kn} = 0, \quad \text{for } k = 1,\ldots,Q^b;$$
$$\boldsymbol{\sigma}_{\overline{Q}^b n} = \zeta_n = \mathbf{u}_h(\boldsymbol{\mu}^n).$$

For $n = N+1,\ldots,2N$:

$$(\boldsymbol{\sigma}_{kn},\mathbf{w})_Y = \mathscr{B}(\xi_{n-N},\mathbf{w})^k, \quad \forall \mathbf{w} \in Y_h, \ \text{for } k = 1,\ldots,\ Q^b; \tag{26}$$
$$\boldsymbol{\sigma}_{\overline{Q}^b n} = 0.$$

In this way we have compacted the reduced basis velocity space made up of velocity (ζ_n) and supremizer solutions ($T^{\boldsymbol{\mu}}\xi_n$).

For a new "$\boldsymbol{\mu}$" we want a solution given by a combination of previously computed stored solutions as basis functions:

$$\mathbf{u}_N(\boldsymbol{\mu}) = \sum_{j=1}^{2N} u_{Nj}(\boldsymbol{\mu}) \left(\sum_{k=1}^{\overline{Q}^b} \Phi^k(\boldsymbol{\mu})\boldsymbol{\sigma}_{kj} \right),$$

$$p_N(\boldsymbol{\mu}) = \sum_{l=1}^{N} p_{Nl}(\boldsymbol{\mu})\xi_l,$$

whose weights u_{Nj} and p_{Nl} are given by the following reduced basis linear system (in this case summation over i and j is no more understood to better explain how to build the on-line system):

$$\begin{cases} \displaystyle\sum_{j=1}^{2N} A_{ij}^{\boldsymbol{\mu}} u_{Nj}(\boldsymbol{\mu}) + \sum_{l=1}^{N} B_{il}^{\boldsymbol{\mu}} p_{Nl}(\boldsymbol{\mu}) = F_i^{\boldsymbol{\mu}}, \quad 1 \leqslant i \leqslant 2N, \\ \displaystyle\sum_{j=1}^{2N} B_{jl}^{\boldsymbol{\mu}} u_{Nj}(\boldsymbol{\mu}) = G_l^{\boldsymbol{\mu}}, \quad 1 \leqslant l \leqslant N, \end{cases} \tag{27}$$

where the sub-matrices $\underline{A}$ and $\underline{B}$ are given by

$$A_{ij}^{\boldsymbol{\mu}} = \sum_{k=1}^{Q^a} \sum_{k'=1}^{\overline{Q}^b} \sum_{k''=1}^{\overline{Q}^b} \Theta^k(\boldsymbol{\mu})\Phi^{k'}(\boldsymbol{\mu})\Phi^{k''}(\boldsymbol{\mu}) \mathscr{A}(\boldsymbol{\sigma}_{k'i},\boldsymbol{\sigma}_{k''j})^k, \quad 1 \leqslant i,j \leqslant 2N,$$

$$B_{il}^{\boldsymbol{\mu}} = \sum_{k=1}^{Q^b} \sum_{k'=1}^{\overline{Q}^b} \Phi^k(\boldsymbol{\mu})\Phi^{k'}(\boldsymbol{\mu}) \mathscr{B}(\boldsymbol{\sigma}_{k'i},\xi_l)^k, \quad 1 \leqslant i \leqslant 2N, \ 1 \leqslant l \leqslant N,$$

and

$$F_i^{\boldsymbol{\mu}} = \sum_{k'=1}^{\overline{Q}^b} \Phi^{k'}(\boldsymbol{\mu}) \langle F, \boldsymbol{\sigma}_{k'i} \rangle, \quad 1 \leqslant i \leqslant 2N;$$
$$G_l^{\boldsymbol{\mu}} = \langle G^0, \xi_l \rangle, \quad 1 \leqslant l \leqslant N.$$

Finally, problem (27) can be written in compact form as

$$\begin{pmatrix} A & B \\ B^{\mathrm{T}} & \mathbf{0} \end{pmatrix} \cdot \begin{pmatrix} \mathbf{u}_N \\ \mathbf{p_N} \end{pmatrix} = \begin{pmatrix} \mathbf{F} \\ \mathbf{G} \end{pmatrix}. \tag{28}$$

This linear system, whose unknowns are the coefficients of the linear combination of previously computed off-line solutions, has the same structure of a finite element Stokes problem. Using reduced basis we deal with a matrix of considerably smaller dimension (of order of N) and with full matrices (instead of sparse ones).

3.1. Reduced basis on-line complexity

We have the following computational costs to build (on-line) reduced basis matrices, given also the supremizer component in the velocity space: $O(Q^a(\overline{Q}^b)^2 4N^2)$ for sub-matrix $\underline{A}$, $O(\overline{Q}^b Q^b 2N^2)$ for $\underline{B}$, $O(\overline{Q}^b 2N)$ for $\underline{F}$ and $O(27N^3)$ for the inversion of the full reduced basis matrix (28). Note that the approach presented to build reduced basis velocity space is only one of the possible solutions and the space $Y_N^{\boldsymbol{\mu}}$, in this case, is depending on the value of the on-line $\boldsymbol{\mu}$ parameter. Other options that avoid ill conditioning problems characterized by different computational costs are available and will be presented in Section 7.

3.2. An application to bypass configuration

After the general presentation of the reduced basis method for Stokes equations we introduce an application of interest used to carry out some preliminary numerical results described in the following sections and to introduce outputs of interest.

In Fig. 1 we represent a "T-bypass" configuration, used, for example, to extract preliminary results about a possible optimized configuration for an arterial bypass and to study

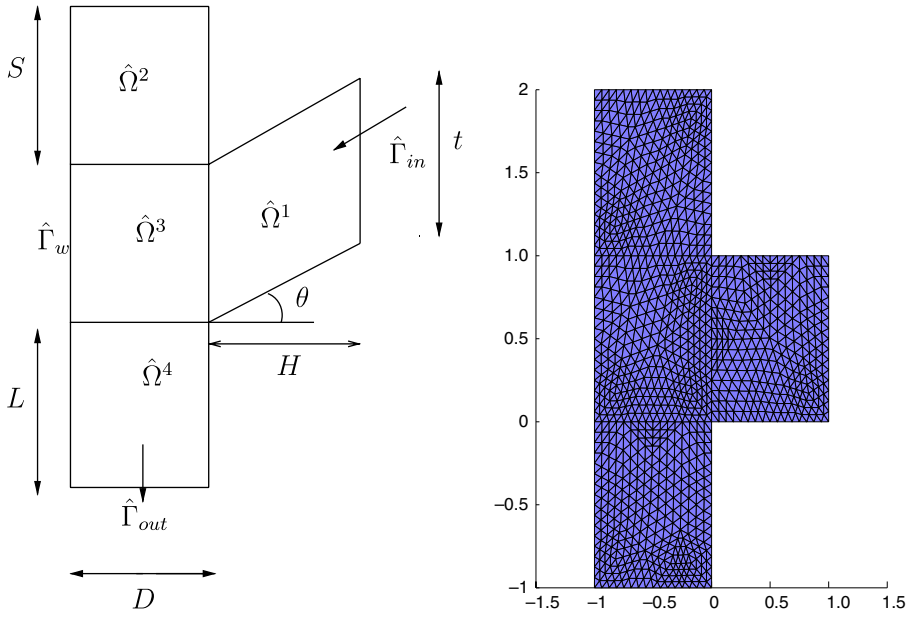

Fig. 1. Physical domain $\widehat{\Omega}$: the four sub-domains and the problem parameters; $\widehat{\Gamma}_{\mathrm{w}} = \widehat{\Gamma} \setminus (\widehat{\Gamma}_{\mathrm{in}} \cup \widehat{\Gamma}_{\mathrm{out}})$ (left). Reference domain Ω (right).

the sensitivity of some geometrical parameters, see also [27].

We introduce a vector of parameters $\boldsymbol{\mu} = \{t, D, L, S, H, \theta\} \in \mathscr{D}^{\mu} \subset \mathbb{R}^P$, $P = 6$, where $\mathscr{D}^{\mu}$ is the Cartesian product: $[t_{\min}, t_{\max}] \times [D_{\min}, D_{\max}] \times [L_{\min}, L_{\max}] \times [S_{\min}, S_{\max}] \times [H_{\min}, H_{\max}] \times [\theta_{\min}, \theta_{\max}]$, representing the range of variation of our parameters of interest during bypass optimization. The physical domain $\widehat{\Omega}$ and the reference one Ω have been divided into four sub-domains ($R = 4$). The *transformation tensors* for the bilinear viscous terms (14):

$$v^r_{ij}(\boldsymbol{\mu}) = G^r_{ii'}(\boldsymbol{\mu}) \hat{v}_{i'j'} G^r_{jj'}(\boldsymbol{\mu}) \det(G^r(\boldsymbol{\mu}))^{-1},$$
$$1 \leqslant i, i', j, j' \leqslant 2, \quad r = 1, \ldots, R,$$

assume this formulation:

$$v^1 = v \begin{bmatrix} \dfrac{t}{H} & -\tan\theta \\ -\tan\theta & \dfrac{1+\tan^2\theta}{t} H \end{bmatrix}; \quad v^2 = v \begin{bmatrix} \dfrac{S}{D} & 0 \\ 0 & \dfrac{D}{S} \end{bmatrix}; \tag{29}$$

$$v^3 = v \begin{bmatrix} \dfrac{t}{D} & 0 \\ 0 & \dfrac{D}{t} \end{bmatrix}; \quad v^4 = v \begin{bmatrix} \dfrac{L}{D} & 0 \\ 0 & \dfrac{D}{L} \end{bmatrix}. \tag{30}$$

The tensors for *pressure and divergence forms* (15):

$$\chi^r_{ij}(\boldsymbol{\mu}) = G^r_{ij} \det(G^r(\boldsymbol{\mu}))^{-1}, \quad 1 \leqslant i, j \leqslant 2, \quad r = 1, \ldots, R$$

are given by

$$\chi^1 = \begin{bmatrix} t & -H\tan\theta \\ 0 & H \end{bmatrix}; \quad \chi^2 = \begin{bmatrix} S & 0 \\ 0 & D \end{bmatrix}; \tag{31}$$

$$\chi^3 = \begin{bmatrix} t & 0 \\ 0 & D \end{bmatrix}; \quad \chi^4 = \begin{bmatrix} L & 0 \\ 0 & D \end{bmatrix}. \tag{32}$$

In this case Q_a and Q_b of (18) and (19) are as large as 32 ($d \times d \times d \times R$) and 16 ($d \times d \times R$), respectively, but due to the fact that the tensors v^r and χ^r have some zero components we have $Q_a = 20$ and $Q_b = 9$. Please note that the tensors v^r should be considered for each component $(u_1, u_2)^{\mathrm{T}}$ of the velocity $\mathbf{u}$.

3.3. Outputs of interest

As outputs of interest we may consider, for example, the mean value of the velocity components:

$$s_1(\boldsymbol{\mu}) = \sum_{r=1}^{R} \frac{\displaystyle\int_{\Omega^r} u_1(\boldsymbol{\mu})\, \mathrm{d}\Omega}{\displaystyle\int_{\Omega^r} \mathrm{d}\Omega};$$
$$s_2(\boldsymbol{\mu}) = \sum_{r=1}^{R} \frac{\displaystyle\int_{\Omega^r} u_2(\boldsymbol{\mu})\, \mathrm{d}\Omega}{\displaystyle\int_{\Omega^r} \mathrm{d}\Omega}. \tag{33}$$

Other outputs are derived from velocity, such as vorticity:

$$s_v(\boldsymbol{\mu}) = \sum_{r=1}^{R} \int_{\Omega_r} \left(\frac{\partial u_2(\boldsymbol{\mu})}{\partial x_1} - \frac{\partial u_1(\boldsymbol{\mu})}{\partial x_2} \right) \mathrm{d}\Omega, \tag{34}$$

or wall shear stress:

$$s_\tau(\boldsymbol{\mu}) = \int_{\Gamma_{\mathrm{w}}} v \frac{\partial \mathbf{u}(\boldsymbol{\mu})}{\partial \hat{\mathbf{n}}} \cdot \hat{\mathbf{t}}\, \mathrm{d}\Gamma, \tag{35}$$

where $\hat{\mathbf{t}}$ is the tangential unit vector. In the last two examples we may introduce a dual residual correction based on an adjoint problem to improve output accuracy (see, for example [29]).

4. Off-line optimized basis assembling: adaptive procedure

An adaptive procedure based on H^1 maximum relative projected error for velocity E_{H^1} has been developed to optimize basis assembling, optionally we can also consider and

combine L^2 maximum relative projected error for pressure E_{L^2}. We underline that, given the higher powers of N that appear in our cost computing estimation, it is crucial (both for on-line and off-line effort) to control N more tightly. To this end, we may gainfully apply an off-line assembling procedure adaptively, see also [34,17]. We first construct, off-line, an approximation that, over most of the domain, exhibits an error ϵ (E_{H^1} or E_{L^2} or both) less than $\epsilon_d^{\text{prior}}$: we begin with a first point $\boldsymbol{\mu}^1$ ($S_{N'=1} = \{\boldsymbol{\mu}^1\}$); we next evaluate error $\epsilon_{N'=1}(\boldsymbol{\mu})$ over a large test sample of parameter points in $\mathscr{D}^{\boldsymbol{\mu}}$, denoted with $\sum^{\text{prior}}$; we then choose for $\boldsymbol{\mu}^2$ (and hence $S_{N'=2} = \{\boldsymbol{\mu}^1, \boldsymbol{\mu}^2\}$) the maximizer of $\epsilon_{N'=1}(\boldsymbol{\mu})$ over $\sum^{\text{prior}}$. We repeat this process until the maximum of $\epsilon_{N'=N^{\text{prior}}}(\boldsymbol{\mu})$ over $\sum^{\text{prior}}$ is lower than $\epsilon_d^{\text{prior}}$. Then, on-line, given a new value of the parameter, $\boldsymbol{\mu}$, and an error tolerance $\epsilon_d^{\text{post}}(\boldsymbol{\mu})$, we essentially repeat this adaptive process – but now our sample points are drawn from $S_{N^{\text{prior}}}$, and the test sample is a singleton – $\boldsymbol{\mu}$. Typically we choose $\epsilon_d^{\text{prior}} \ll \epsilon_d^{\text{post}}(\boldsymbol{\mu})$ since our test is not exhaustive; and therefore, typically, $N^{\text{post}}(\boldsymbol{\mu}) \ll N^{\text{prior}}$. With the adaptive process we get higher accuracy at lower N: modest reductions in N can translate into measurable performance improvements. This procedure is very important not only to get a computationally cheaper and faster procedure but also to avoid ill conditioning in matrix assembling procedures. Error projection procedure, described below, has permitted us to have an off-line adaptive (and optimized) assembling procedure which is very fast and inexpensive, without reduced basis matrix assembling procedures, but based only on the solution of a linear system.

4.1. L^2 pressure error projection

Given a new $\boldsymbol{\mu}$ and hence a new approximated $p_h(\boldsymbol{\mu})$ pressure solution we solve the following linear system:

$$\sum_j^N \int_\Omega \xi_i \xi_j c_j \,\mathrm{d}\Omega = \int_\Omega \xi_i p_h(\boldsymbol{\mu})\,\mathrm{d}\Omega, \quad 1 \leqslant i \leqslant N, \tag{36}$$

where ξ_i are N pressure solutions used as basis given by $\xi_i = \sum_{k=1}^{\mathscr{N}_P} p_{i_k} \Phi_k$, computed solving a finite element problem on $\mathscr{N}_P$ pressure nodes of the mesh; Φ_k are finite element local functions for the pressure. Expanding (36) by finite element approximation we can write

$$\sum_{j=1}^{N} \sum_{l=1}^{\mathscr{N}_P} \sum_{k=1}^{\mathscr{N}_P} p_{i_l} \left(\int_\Omega \Phi_l \Phi_k \,\mathrm{d}\Omega \right) p_{j_k} c_j = \sum_{m=1}^{\mathscr{N}_P} \sum_{n=1}^{\mathscr{N}_P} p_{i_m} \left(\int_\Omega \Phi_m \Phi_n \,\mathrm{d}\Omega \right) p_{h_n}(\boldsymbol{\mu}), \quad 1 \leqslant i \leqslant N,$$

and using compact notation:

$$(\mathbf{p}_i^{\mathrm{T}} M^p \mathbf{p}_j)\mathbf{c} = \mathbf{p}_i^{\mathrm{T}} M^p \mathbf{p}_h(\boldsymbol{\mu}),$$
$$\widehat{M}^p \mathbf{c} = \mathbf{F}^p.$$

Once we have $\mathbf{c}$ we write the L^2 pressure error E_{L^2} as

$$E_{L^2}^2 = \|p_h(\boldsymbol{\mu})\|_{L^2}^2 - \sum_{i=1}^{N} \sum_{j=1}^{N} c_i \left(\int_\Omega \xi_i \xi_j \,\mathrm{d}\Omega \right) c_j,$$

where $(\int_\Omega \xi_i \xi_j \,\mathrm{d}\Omega)$ is the *pressure mass* matrix $\widehat{M}_{ij}^p = \sum_{l=1}^{\mathscr{N}_P} \sum_{k=1}^{\mathscr{N}_P} p_{i_l} (\int_\Omega \Phi_l \Phi_k \,\mathrm{d}\Omega) p_{j_k}$, $1 \leqslant i, \quad j \leqslant N$, i.e., $\mathbf{p}_i^{\mathrm{T}} M^p \mathbf{p}_j$.

4.2. H^1 velocity error projection

Given a new $\boldsymbol{\mu}$ and hence a new approximated velocity solution $u_h(\boldsymbol{\mu})$ we solve the following linear system

$$\sum_j^{2N} \left(\int_\Omega \zeta_i \zeta_j \,\mathrm{d}\Omega + \int_\Omega \nabla\zeta_i \cdot \nabla\zeta_j \,\mathrm{d}\Omega \right) c_j = \int_\Omega \zeta_i u_h(\boldsymbol{\mu})\,\mathrm{d}\Omega + \int_\Omega \nabla\zeta_i \cdot \nabla u_h(\boldsymbol{\mu})\,\mathrm{d}\Omega, \quad 1 \leqslant i \leqslant 2N, \tag{37}$$

where ζ_i are $2N$ velocity solutions used as basis, made up of finite element approximated velocities and supremizer solutions, written as $\zeta_i = \sum_{k=1}^{\mathscr{N}} u_{i_k} \Psi_k$ on $\mathscr{N}$ velocity nodes by Ψ_k finite element velocity local functions. Expanding the system (37) by finite element approximation (on $\mathscr{N}$ nodes) we get, for $1 \leqslant i \leqslant 2N$:

$$\left[\sum_{j=1}^{2N} \sum_{l=1}^{\mathscr{N}} \sum_{k=1}^{\mathscr{N}} u_{i_l} \left(\int_\Omega \Psi_l \Psi_k \,\mathrm{d}\Omega \right) u_{j_k} + \sum_{j=1}^{2N} \sum_{l=1}^{\mathscr{N}} \sum_{k=1}^{\mathscr{N}} u_{i_l} \left(\int_\Omega \nabla\Psi_l \cdot \nabla\Psi_k \,\mathrm{d}\Omega \right) u_{j_k} \right] c_j = \sum_{m=1}^{\mathscr{N}} \sum_{n=1}^{\mathscr{N}} u_{i_m} \left(\int_\Omega \Psi_m \Psi_n \,\mathrm{d}\Omega \right) u_{h_n}(\boldsymbol{\mu}) + \sum_{m=1}^{\mathscr{N}} \sum_{n=1}^{\mathscr{N}} u_{i_m} \left(\int_\Omega \nabla\Psi_m \cdot \nabla\Psi_n \,\mathrm{d}\Omega \right) u_{h_n}(\boldsymbol{\mu}),$$

and in compact notation:

$$(\mathbf{u}_i^{\mathrm{T}}(M+K)\mathbf{u}_j)\mathbf{c} = \mathbf{u}_i^{\mathrm{T}}(M+K)\mathbf{u}_h(\boldsymbol{\mu}),$$
$$\widehat{M}^u \mathbf{c} = \mathbf{F}^u.$$

Once we have $\mathbf{c}$ we write the H^1 velocity error E_{H^1} as

$$E_{H^1}^2 = \|u_h(\boldsymbol{\mu})\|_{H^1}^2 - \sum_{i=1}^{2N} \sum_{j=1}^{2N} c_i \left(\int_\Omega \zeta_i \zeta_j \,\mathrm{d}\Omega + \nabla\zeta_i \cdot \nabla\zeta_j \,\mathrm{d}\Omega \right) c_j,$$

where $(\int_\Omega \zeta_i \zeta_j \,\mathrm{d}\Omega)$ is the *velocity mass* matrix $\sum_{l=1}^{\mathscr{N}} \sum_{k=1}^{\mathscr{N}} u_{i_l} (\int_\Omega \Psi_l \Psi_k \,\mathrm{d}\Omega) u_{j_k}$, i.e., $\mathbf{u}_j^{\mathrm{T}} M \mathbf{u}_i$ and $(\int_\Omega \nabla\zeta_i \cdot \nabla\zeta_j \,\mathrm{d}\Omega) = \sum_{l=1}^{\mathscr{N}} \sum_{k=1}^{\mathscr{N}} u_{i_l} (\int_\Omega \nabla\Psi_l \cdot \nabla\Psi_k \,\mathrm{d}\Omega) u_{j_k}$ the *velocity stiffness* matrix, i.e., $\mathbf{u}_j^{\mathrm{T}} K \mathbf{u}_i$.

5. The computation of the constant β of the inf–sup condition

The calculation of the constant of the inf–sup condition for finite element (β) and reduced basis method (β_N) has been carried out as a test to guarantee approximation stability:

- β is related to the generalized eigenvalue problem (see [7,13,23]):

$$S\mathbf{z} = \lambda M^p \mathbf{z} \tag{38}$$

Table 1
The constants β and β_N for several values of the parameter D

D	β	β_N, $N=1$	β_N, $N=2$	β_N, $N=3$
0.63	2.0249	3.9096	2.7895	2.531
0.68	2.0286	3.9316	2.8708	2.6625
0.73	2.0274	3.952	2.9456	2.7992
0.78	2.0257	3.971	3.0145	2.9386
0.83	2.0237	3.9888	3.0781	3.0729
0.88	2.0216	4.0054	3.137	3.0729
0.93	2.0192	4.0208	3.1918	3.186
0.98	2.0167	4.0353	3.243	3.264
1.03	2.0139	4.0487	3.291	3.3466
1.08	2.011	4.0612	3.3361	3.3759

Other parameters are frozen.

where $S = G^{\mathrm{T}}K^{-1}G$, K is the finite element (velocity) stiffness matrix ($\int_\Omega \nabla\Psi_l \cdot \nabla\Psi_k \,\mathrm{d}\Omega$), G is the velocity-divergence finite element matrix ($\int_\Omega \Phi_l \nabla\cdot\Psi_k \,\mathrm{d}\Omega$), M^p is the finite element pressure mass matrix ($\int_\Omega \Phi_l\Phi_k \,\mathrm{d}\Omega$). Precisely, β is given by

$$\beta = \sqrt{\lambda_{\min}}; \tag{39}$$

S is symmetric and positive definite and its eigenvalues are real and positive.

- To calculate β_N we have a generalized eigenvalues problem on reduced basis (full) matrices (previously defined):

$$S_N \mathbf{z}_N = \lambda_N \widehat{M}^p \mathbf{z}_N \tag{40}$$

with $S_N = B^{\mathrm{T}}A^{-1}B$ symmetric and positive definite, whose eigenvalues are real and positive. This time

$$\beta_N = \sqrt{\lambda_{N_{\min}}}. \tag{41}$$

- We have tested that the inequalities: $\beta_N(\boldsymbol{\mu}) \geqslant \beta(\boldsymbol{\mu}) \geqslant \beta_0 > 0, \forall \boldsymbol{\mu} \in \mathscr{D}^{\boldsymbol{\mu}}$ are satisfied. Table 1 shows a test driven to calculate the constant β of the *inf–sup* condition studying a one-parameter varying configuration (the parameter D, for example) for different N.

6. Some preliminary numerical results

Several numerical tests were carried out to develop all the Stokes reduced basis toolbox and to study different related aspects: affine mapping transformation in reference domains, off-line optimization for basis assembling procedure, approximation and algebraic stability (inf–sup condition fulfillment and condition number control). Different meshes have been used (from coarse to fine). Using finer mesh the CPU time (on a Pentium IV, 2 GHz) increases a lot during computational procedures such as off-line calculations, i.e., reduced basis approximation spaces and matrix assembling, error estimation and, eventually, orthonormalization, but it is maintained reasonable during on-line calculation. A mesh adaptation procedure in some zones has been implemented. Taylor–Hood $\mathbb{P}^2 - \mathbb{P}^1$ elements (for velocity and pressure respectively) have been used [23]. Different solver for finite element and reduced basis systems have been used: both iterative (such as *Bi-CGSTAB*, *Conjugate Gradient Method*, *GMRES*) and direct, see [22]. The reduced basis solutions have been compared directly with the true finite element solutions by computing H^1 relative error for velocity and L^2 relative error for pressure.

6.1. First test: homogeneous Dirichlet boundary conditions, forced flow, three varying parameters

The first test we introduce deals with a forced Stokes flow in the domain considered with all zero Dirichlet boundary conditions (flow in a cavity), varying only three parameters available (depending by one non-dimensional quantity denoted with τ). Data and relationships for geometrical parameters used to solve the problem follow (see also Fig. 1).

(I) The varying parameters are $t = 3 - 2\tau$, $S = \tau$ and $L = \tau$.
(II) The viscosity is $\nu = 0.04\,\mathrm{m}^2\,\mathrm{s}^{-1}$, the force field is $\hat{\mathbf{f}} = (0, 10x_1)^{\mathrm{T}}\,\mathrm{m\,s}^{-2}$ in the physical domain $\widehat{\Omega}$.
(III) The non-dimensional parameter τ is ranging in $[0.1, 1.45]$. All other parameters are frozen: $H = 1$, $D = 1$ and the angle $\theta = 0$.

Fig. 2 shows examples of flow solutions: velocity (absolute value) for two configurations with $\tau_{\min}$ and $\tau_{\max}$; Fig. 3 shows the error reduction using the adaptive optimized procedure of Section 4 during basis assembling procedure, based on H^1 relative (projected) error minimization, on the left, and the parameters distribution during basis assembling procedure, on the right. Fig. 4 shows true relative error reduction (H^1 for velocity and L^2 for pressure) considering a great number of different geometrical configurations. Table 2 shows error reduction (and its magnitude); Table 3 shows the proofs of approximation stability of reduced basis formulation computing β_N, the inf–sup equivalent constant and its comparison with β from Galerkin (FEM) approximation. Fig. 5 shows the error on a possible output of interest, for example $s(\boldsymbol{\mu}) = \int_\Omega \mathbf{f}\cdot\mathbf{u}(\boldsymbol{\mu})\,\mathrm{d}\Omega$.

6.2. Second test: mixed Dirichlet/Neumann boundary conditions, five varying parameters

The second test deals with a flow in the considered domain imposing Neumann homogeneous boundary conditions on inflow Γ_{in} and outflow Γ_{out} and homogeneous Dirichlet condition on the wall Γ_{w}. We deal with five varying parameters (bound by three relationships depending on two non-dimensional quantities τ and ρ), only θ is fixed to zero. Data and values used follow:

- The parameters are $t = 3 - 2\tau$, $S = \tau$, $L = \tau$, $D = \rho$ and $H = 2 - \rho$.

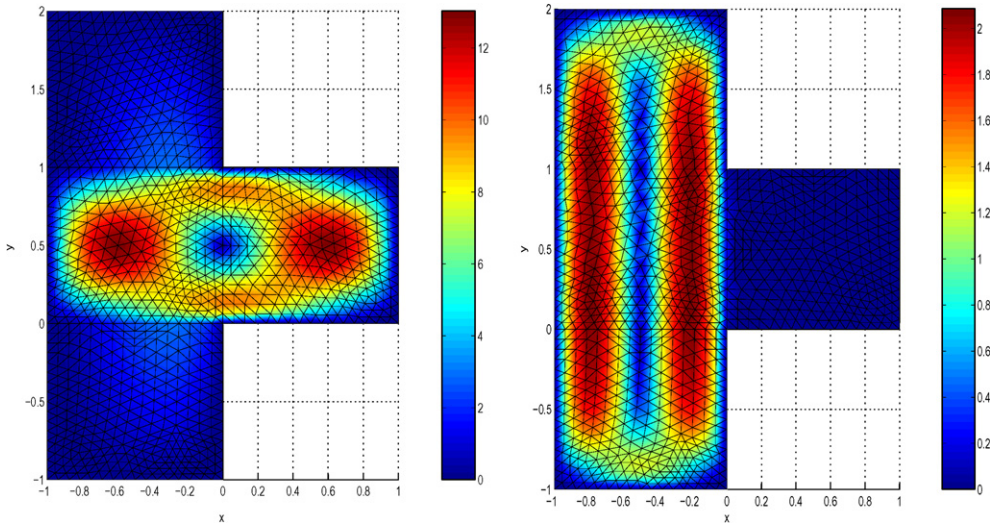

Fig. 2. Velocity solution (absolute value) for $\tau = 0.1$ (left) and $\tau = 1.45$ (right), m s$^{-1} \times 10^{-2}$.

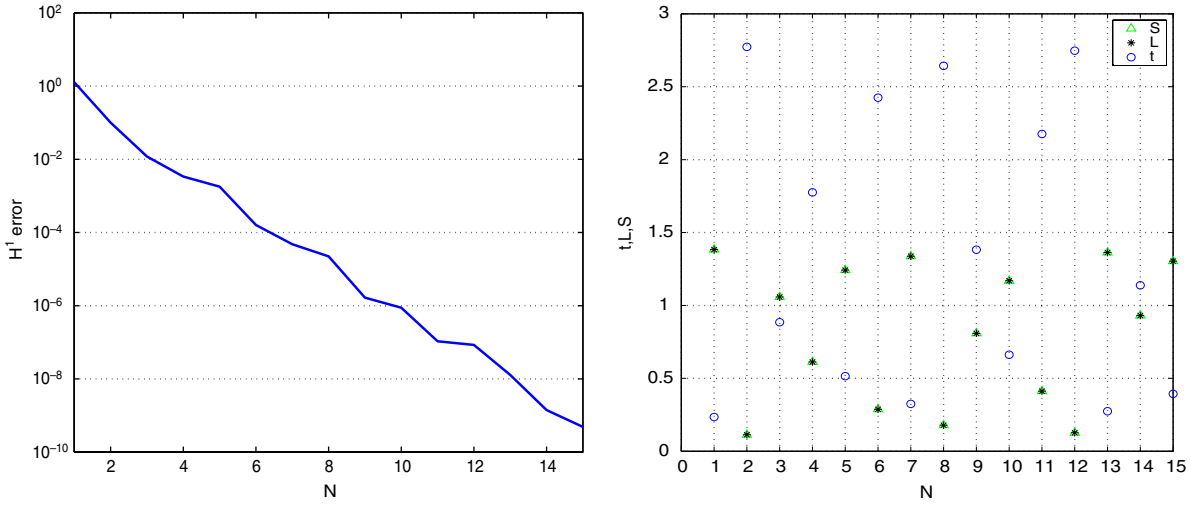

Fig. 3. Left: maximum H^1 relative projected error (see Section 4.2) on velocity at each iteration during adaptive basis assembling. Right: parameters distribution during off-line reduced basis assembling procedure (D and H are fixed).

- The viscosity is $0.04\,\mathrm{m}^2\,\mathrm{s}^{-1}$, while the force field is $\mathbf{f} = (0, 10)^{\mathrm{T}}\,\mathrm{m\,s}^{-2}$ in true domain $\widehat{\Omega}$.
- The parameters range is $\tau \in [0.1, 1.45]$ and $\rho \in [0.1, 1.9]$.

Fig. 6 shows an example of flow solution (velocity absolute value) for a certain parameters combination ($\rho = \tau = 1.0$); Fig. 7 shows on the left the off-line parameters distribution during basis assembling procedures based on the reduction of the H^1 relative projected error using the adaptive procedure; on the right we have maximum and mean output error Δs over a large number of different configurations, considering, for example, $s(\boldsymbol{\mu}) = \int_{\Omega} \mathbf{f} \cdot \mathbf{u}(\boldsymbol{\mu})\, \mathrm{d}\Omega$. Fig. 8 shows the true relative error reduction (H^1 for velocity and L^2 for pressure) considering a great number of different geometrical configurations. Table 4 shows error reduction (and its magnitude) and Table 5 the errors over the output of interest.

6.3. Third test: homogeneous Dirichlet boundary conditions, forced flow, six varying parameters

The third test we carried out considered a forced Stokes flow in the domain imposing all zero Dirichlet boundary conditions, varying all the six parameters available (depending by two non-dimensional quantities: τ, ρ), including the angle θ. Data and relationship used in this test are reported below:

- The parameters are $t = 3 - 2\tau$, $S = \tau$, $L = \tau$, $D = \rho$, $H = 2 - \rho$ and the angle is θ.
- The viscosity is $0.04\,\mathrm{m}^2\,\mathrm{s}^{-1}$, the force field is $\hat{\mathbf{f}} = (0, 10x_1)^{\mathrm{T}}\,\mathrm{m\,s}^{-2}$ in the true domain $\widehat{\Omega}$.
- The parameters range are $\tau \in [0.1, 1.45]$, $\rho \in [0.1, 1.9]$ and for the angle $\theta \in [0, \pi/3]$.

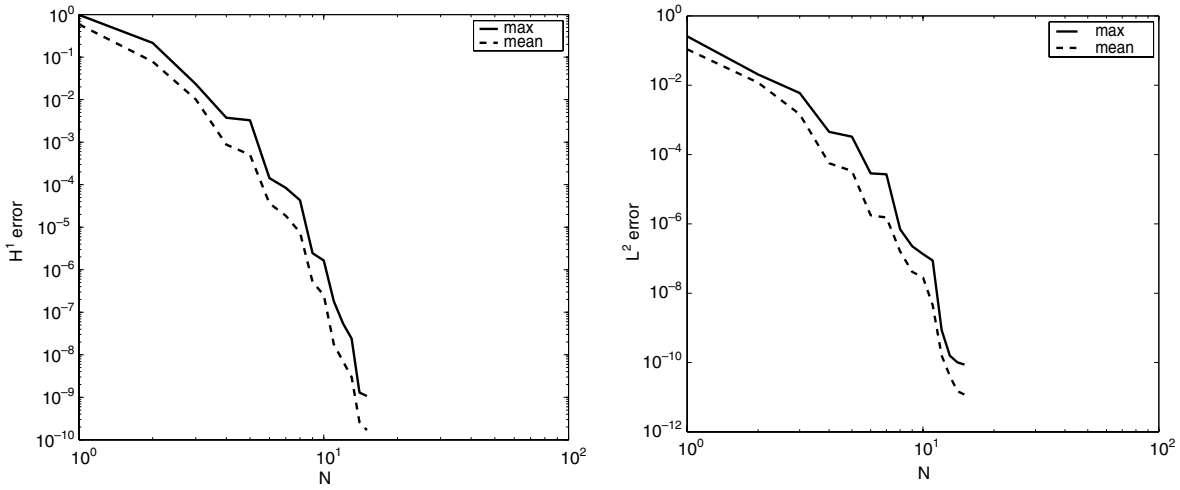

Fig. 4. Left: H^1 relative errors on velocity, maximum and mean values over a large test sampling (50 configurations). Right: relative L^2 pressure errors, maximum and mean values over a large test sampling (50 configurations); errors in log–log scale.

Table 2
Table of H^1 and L^2 relative errors on velocity and pressure, respectively, 50 test configurations, three parameters varying

N	Relative error H^1 max	Relative error H^1 mean	Relative error L^2 max	Relative error L^2 mean
1	9.8900e−001	5.9138e−001	2.5790e−001	1.0878e−001
2	2.1583e−001	7.8312e−002	2.0387e−002	1.1826e−002
3	2.3301e−002	1.0174e−002	5.9742e−003	1.4583e−003
4	3.7543e−003	8.7714e−004	4.4999e−004	5.5973e−005
5	3.2670e−003	5.0383e−004	3.2752e−004	3.3635e−005
6	1.4271e−004	3.6446e−005	2.8591e−005	1.7688e−006
7	8.4314e−005	1.8559e−005	2.7009e−005	1.5313e−006
8	4.3142e−005	7.4860e−006	7.0025e−007	1.6084e−007
9	2.4504e−006	5.2102e−007	2.2660e−007	4.1354e−008
10	1.6485e−006	2.5155e−007	1.3400e−007	2.8537e−008
11	1.8195e−007	1.7635e−008	8.8023e−008	4.5140e−009
12	5.3852e−008	6.9109e−009	8.6392e−010	1.5917e−010
13	2.4053e−008	2.9963e−009	1.5813e−010	4.1002e−011
14	1.2923e−009	2.5982e−010	1.0129e−010	1.4957e−011
15	1.0702e−009	1.6946e−010	8.7277e−011	1.1840e−011

Table 3
β_N equivalent inf–sup constant

N	β_N	N	β_N	N	β_N
1	6.5012e+000	6	5.7051e+000	11	5.6263e+000
2	5.8811e+000	7	5.7048e+000	12	5.6245e+000
3	5.7978e+000	8	5.7047e+000	13	5.6087e+000
4	5.7876e+000	9	5.7056e+000	14	5.5935e+000
5	5.7344e+000	10	5.6309e+000	15	5.4651e+000

$\beta = 5.0164$ ($\tau = 0.76$).

Fig. 9 shows the projected error reduction (as shown in Section 4.2) using the adaptive procedure in basis assembling, based on H^1 error minimization and parameters distribution during basis assembling procedure. Fig. 10 shows true error reduction (H^1 for velocity and L^2 for pressure) considering a great number of different geometrical configurations. The plateau in pressure error plot is due to the fact that we are optimizing reduced basis velocity approximation space with adaptive procedures, but nothing is done with pressure. Table 6 shows error reduction (and its magnitude) and Table 7 the error on an output of interest: $s(\boldsymbol{\mu}) = \int_\Omega \mathbf{f} \cdot \mathbf{u}(\boldsymbol{\mu})\, d\Omega$. A second option is carried out using and adaptive off-line procedure based on total projected error (velocity and pressure). Fig. 11 shows projected error reduction using the adaptive procedure during basis assembling. Fig. 12 shows error reduction (H^1 for velocity and L^2 for pressure) considering different geometrical configurations. In this case the plateau in the pressure error behavior disappears because we are optimizing reduced basis velocity and pressure approximation spaces with adaptive procedures minimizing off-line error.

6.4. On computational costs

In Table 8 we report some on-line computational costs (CPU time) versus N. The finite element solution is obtained with a mean CPU time of 112.23, adopting a

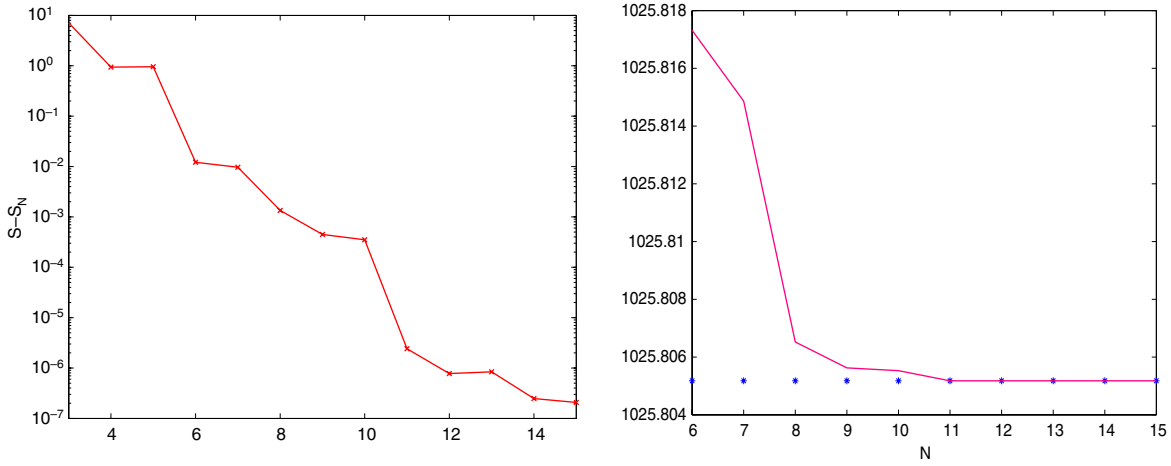

Fig. 5. Left: error on functional output $\Delta s = (s - s_N)$; $s = \int_\Omega \mathbf{f} \cdot \mathbf{u} \mathrm{d}\Omega$. Right: convergence of s_N to s $(*)$ versus N $(\tau = 0.356)$.

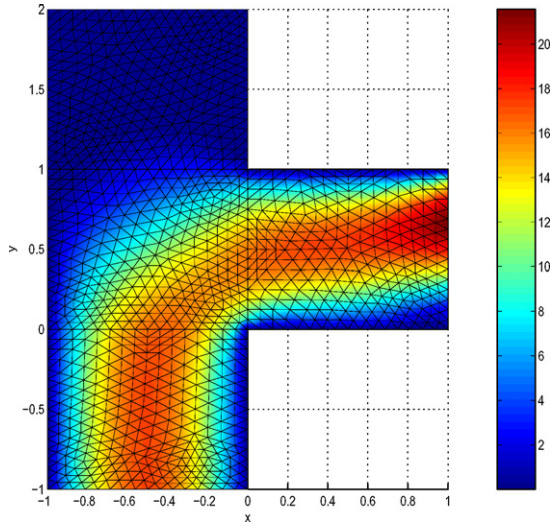

Fig. 6. Example of flow solution (velocity absolute value, m $s^{-1} \times 10^{-2}$) in the parametrized domain.

mesh with 1278 elements, see Fig. 1. Note the computational savings in the on-line step once we have assembled reduced basis matrix. In the same table we have inserted H^1 error indication to compare the computational costs and precision reached. The example refers to the case of a single varying parameter D.

7. On algebraic and approximation stability

To control the condition number of reduced basis matrix we have adopted an orthonormalization procedure applied to velocity and pressure basis functions. After orthonormalization (to achieve algebraic stability) we have to satisfy the approximation stability condition on β_N, the equivalent reduced basis *inf–sup* constant. But if we apply the orthonormalization algorithm to reduced basis approximation spaces, assembled as proposed in Section 3, we may lose the validity of Lemma 3.1 to guarantee the

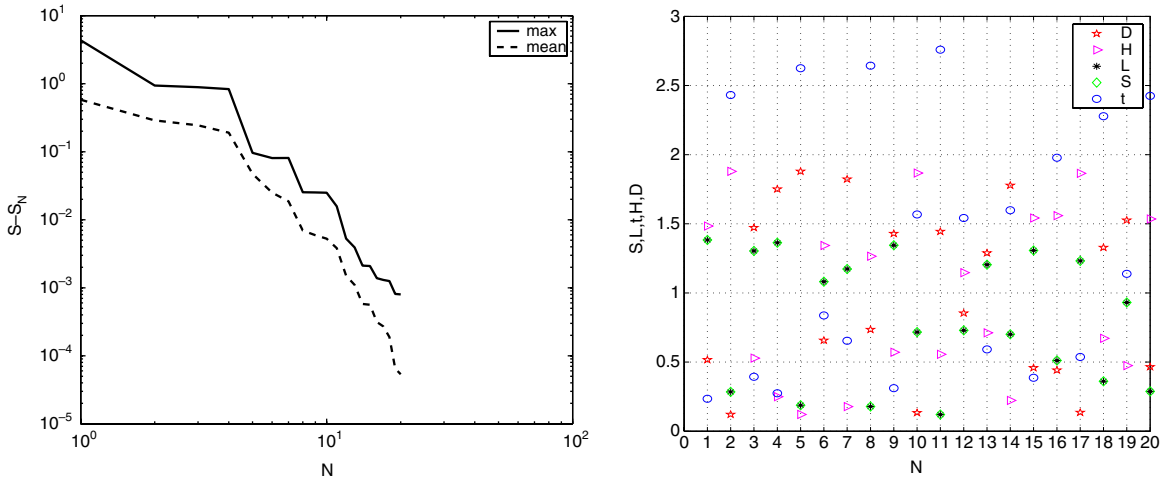

Fig. 7. Left: functional output error $\Delta s = (s - s_N)$; $s = \int_\Omega \mathbf{f} \cdot \mathbf{u} \mathrm{d}\Omega$: maximum and mean error over large test sample configurations. Right: parameters distribution during off-line reduced basis optimized assembling procedure.

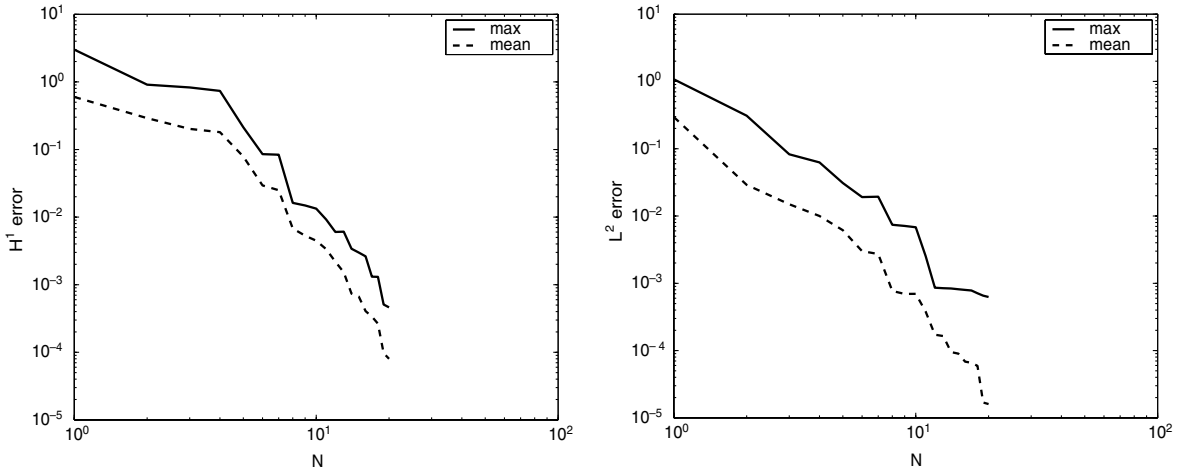

Fig. 8. Left: relative H^1 velocity errors: maximum and mean values over a large test sampling (50 configurations). Right: relative L^2 pressure errors: maximum and mean values over a large test sampling (50 configurations); errors in log–log scale.

Table 4
Table of H^1 relative errors on velocity and L^2 relative errors on pressure, 50 test configurations, five varying parameters, $N \leqslant 20$

N	Relative error H^1 max	Relative error H^1 mean	Relative error L^2 max	Relative error L^2 mean
5	2.93e−001	7.86e−002	3.09e−002	6.14e−003
10	1.33e−002	4.47e−003	6.79e−003	6.96e−004
15	2.98e−003	6.65e−004	8.16e−004	9.021e−005
20	4.61e−004	8.01e−005	6.24e−004	1.60e−005

Table 5
$\Delta s = s - s_N$ max and mean error over output s for 50 configurations

N	Δs max	N	Δs mean
5	9.62e−002	5	4.73e−002
10	2.49e−002	10	5.27e−003
15	2.09e−003	15	5.63e−004
20	7.68e−004	20	5.35e−005

stability of the approximation. For this reason we are going to propose other options in building the reduced basis velocity space.

7.1. Orthonormalization: Gram–Schmidt (GS) algorithm

We recall very briefly the main step of GS orthonormalization:

- Given: $\mathbf{z}_j$, $j = 1, \ldots, N$ a family vector of functions;
- we obtain $\mathbf{l}_j = \frac{P_j \mathbf{z}_j}{\|P_j \mathbf{z}_j\|}$, where P_j is an orthogonal projector onto the orthogonal complement of $\langle \mathbf{l}_1, \mathbf{l}_2, \ldots, \mathbf{l}_{j-1} \rangle$ (i.e., the space generated by $\mathbf{l}_v$ for $v = 1, \ldots, j-1$).
- Each $\mathbf{l}_j$ is orthogonal to $\mathbf{l}_1, \mathbf{l}_2, \ldots, \mathbf{l}_{j-1}$ and lies in $\langle \mathbf{z}_1, \mathbf{z}_2, \ldots, \mathbf{z}_j \rangle$.

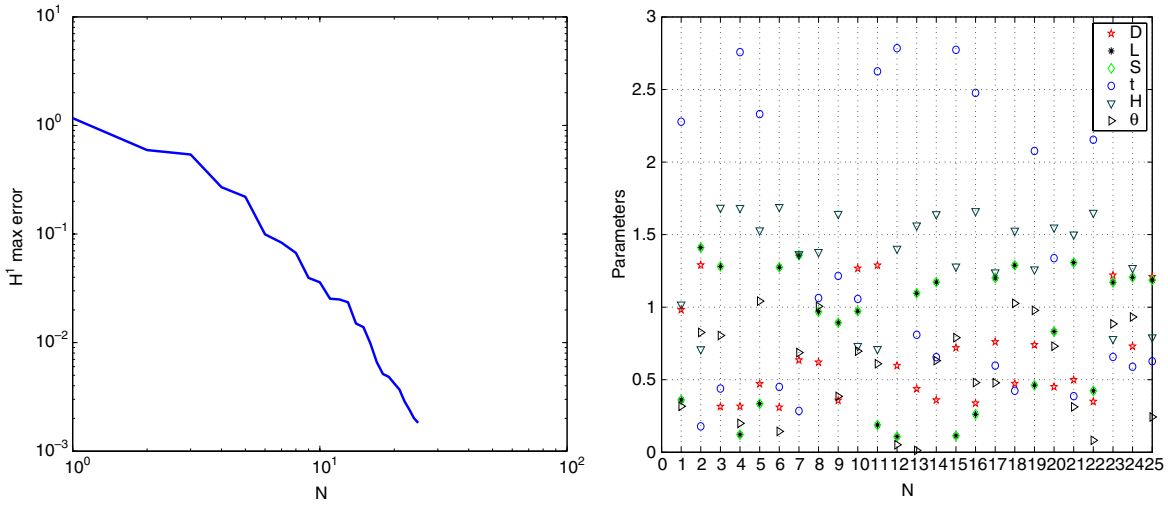

Fig. 9. Left: H^1 velocity (projected) error reduction during basis assembling. Right: parameters distribution during off-line reduced basis assembling.

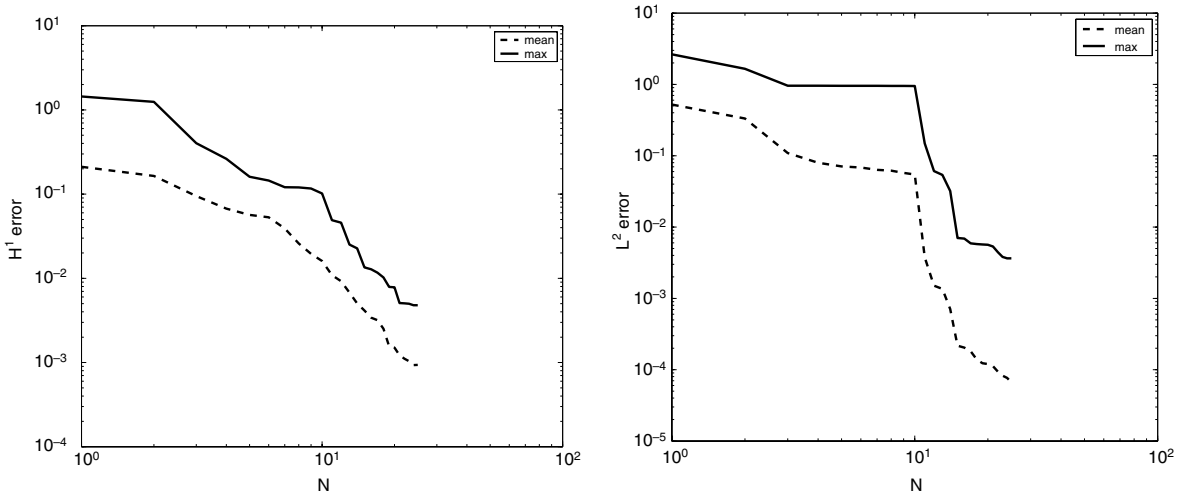

Fig. 10. Left: relative H^1 velocity errors: maximum and mean values over a large test sampling (90 configurations.). Right: relative L^2 pressure errors: maximum and mean error over a large test sampling (90 configurations); errors in log–log scale.

Table 6
Table of velocity relative errors H^1 and pressure L^2, 90 test configurations, 6(3) parameters, $N \leqslant 25$

N	Relative error H^1 max	Relative error H^1 mean	Relative error L^2 max	Relative error L^2 mean
5	1.60e−001	5.65e−002	9.55e−001	7.08e−002
10	1.01e−001	1.60e−002	9.48e−001	5.74e−002
15	1.348e−002	4.14e−003	7.02e−003	2.17e−004
20	7.82e−003	1.49e−003	5.64e−003	1.20e−004
25	4.79e−003	9.37e−004	3.63e−003	6.66e−005

Table 7
Maximum and mean error on functional output $\Delta s = (s - s_N)$: $s = \int_\Omega \mathbf{f} \cdot \mathbf{u} \mathrm{d}\Omega$ for 90 configurations

N	Δs max	N	Δs mean
5	1.34e−001	5	3.26e−002
10	1.26e−001	10	6.91e−003
15	4.064e−003	15	6.87e−004
20	2.50e−003	20	2.92e−004
25	1.38e−003	25	2.31e−004

- Each $\|\mathbf{l}_j\| = 1$.
- $P_j = I - L_{j-1} L_{j-1}^{\mathrm{T}}$; $L_{j-1} = \{\mathbf{l}_1, \ldots, \mathbf{l}_{j-1}\}$;
- $P_j \mathbf{z}_j = \mathbf{z}_j - (\mathbf{l}_1^{\mathrm{T}} \mathbf{l}_j)\mathbf{l}_1 - (\mathbf{l}_2^{\mathrm{T}} \mathbf{z}_j)\mathbf{l}_2 - \ldots - (\mathbf{l}_{j-1}^{\mathrm{T}} \mathbf{z}_{j-1})\mathbf{l}_{j-1}$;
- $\{\mathbf{l}_1, \ldots, \mathbf{l}_N\}$ is an orthogonal basis of $\langle \mathbf{z}_1, \mathbf{z}_2, \ldots, \mathbf{z}_N \rangle$.

The norm $\|\cdot\|$ used here is the $Y = (H^1(\Omega))^2$ for velocity (and supremizers) and $L^2(\Omega)$ for pressure. The scalar product $\mathbf{l}_i^{\mathrm{T}} \mathbf{z}_j$ is the one induced by the functional space and the norm we use. The orthonormalization procedure has been applied to reduced basis functions. For velocity and pressure the procedure is standard. For the supremizer we have to introduce some considerations. Referring to previous supremizer formulation of (26) and to the compact notation already introduced in the reference domain, thanks to the linearity of supremizer operator and to the affine composition property we have for $n = N + 1, \ldots, 2N$:

$$(\boldsymbol{\sigma}_n, \mathbf{v})_{H^1} = \sum_{q=1}^{Q^b} \Phi^q(\boldsymbol{\mu})(\boldsymbol{\sigma}_{qn}, \mathbf{v})_{H^1} = \sum_{q=1}^{Q^b} \Phi^q(\boldsymbol{\mu}) \mathscr{B}(\xi_{n-N}, \mathbf{v})^q, \quad \forall \mathbf{v} \in (H^1_{\Gamma_D}(\Omega))^2,$$

in fact

$$(\boldsymbol{\sigma}_n, \mathbf{v})_{H^1} = \mathscr{B}(\boldsymbol{\mu}; \xi_{n-N}, \mathbf{v}), \tag{42}$$

but we recall that for each q component it holds

$$(\boldsymbol{\sigma}_{qn}, \mathbf{v})_{H^1} = \mathscr{B}(\xi_{n-N}, \mathbf{v})^q \tag{43}$$

and by the affine composition/decomposition of the operator we write

$$\mathscr{B}(\boldsymbol{\mu}; \xi, \mathbf{v}) = \sum_{q=1}^{Q^b} \Phi^q(\boldsymbol{\mu}) \mathscr{B}(\xi, \mathbf{v})^q.$$

At this point we have two possibilities (referring to nth supremizer σ_n, $n = N + 1, \ldots, 2N$) in applying orthonormalization: (i) an orthonormalization (GS) directly on $\boldsymbol{\sigma}_n$ done on-line (being $\boldsymbol{\sigma}_n$ dependent on $\boldsymbol{\mu}$) to obtain $\boldsymbol{\sigma}_n^{\perp}$ as new element (basis function) to enrich the reduced basis velocity space:

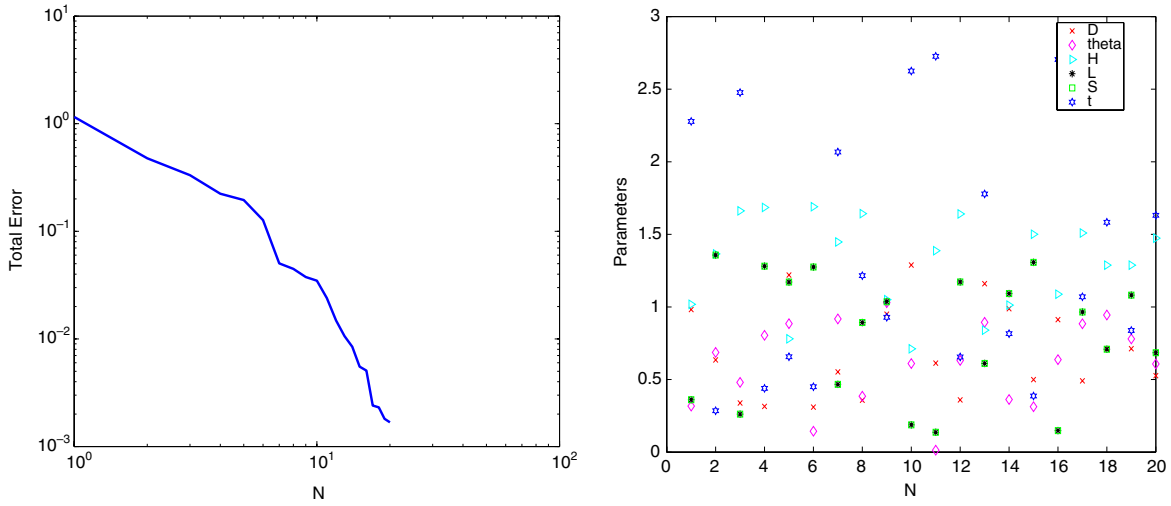

Fig. 11. Left: H^1 velocity and L^2 pressure (projected) errors reduction during basis assembling. Right: corresponding parameters distribution during off-line reduced basis assembling.

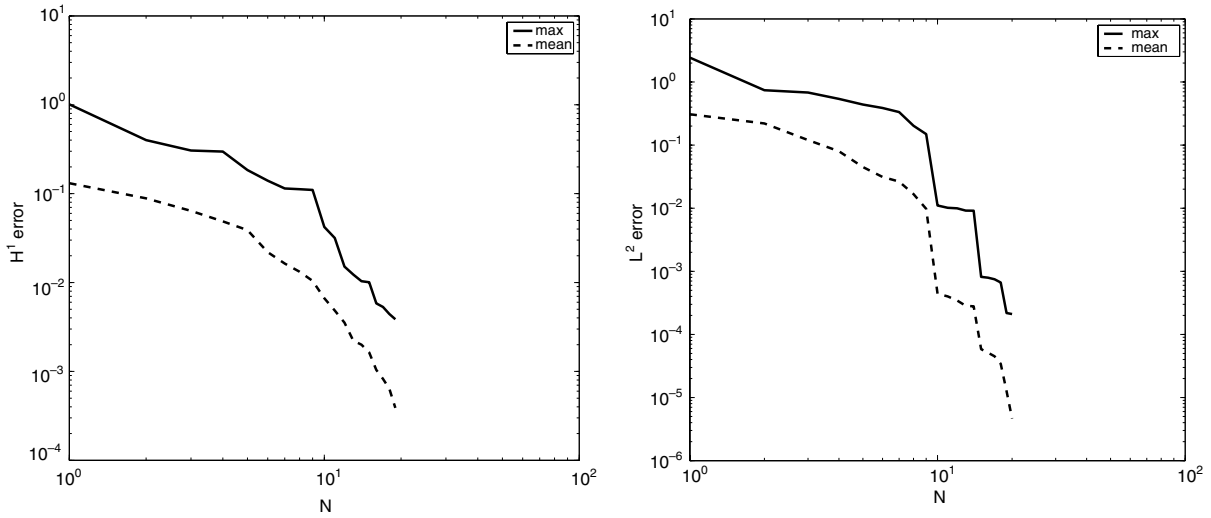

Fig. 12. Left: relative H^1 velocity errors: maximum and mean error over a large test sampling (90 configurations). Right: relative L^2 pressure errors: maximum and mean error over a large test sampling (90 configurations); errors in log–log scale.

Table 8
On-line computational costs (CPU time) varying N (and H^1 velocity error) and comparison with computational cost of FEM solution (%)

N	CPU time	H^1 error	%	N	CPU time	H^1 error	%
1	1.597	6.24e−1	1.4	2	2.445	2.16e−1	2.2
3	3.225	6.58e−3	2.9	4	4.937	5.30e−4	4.4
5	5.908	1.92e−4	5.2	6	5.908	1.006e−4	5.2
7	6.68	5.27e−5	5.9	8	7.55	3.36e−5	6.7
9	8.442	6.83e−7	7.52	10	9.314	1.11e−7	8.3
11	10.615	2.66e−8	9.45	12	14.11	1.98e−8	12.57
13	14.38	1.25e−8	12.81	14	17.895	2.91e−12	15.9
15	20.601	1.38e−12	18.4	16	24.646	4.05e−13	21.9
17	24.625	2.20e−13	21.9	18	23.614	2.74e−14	21.1
19	24.025	2.19e−14	21.4	20	25.257	1.39e−15	22.5

$$\boldsymbol{\sigma}_n^{\perp} = \frac{P_n^{\perp}\boldsymbol{\sigma}_n}{\|P_n^{\perp}\boldsymbol{\sigma}_n\|},$$

$$\boldsymbol{\sigma}_n^{\perp} = \frac{P_n^{\perp}\left(\sum_{q=1}^{Q^b}\Phi_q(\boldsymbol{\mu})\boldsymbol{\sigma}_{qn}\right)}{\|P_n^{\perp}\left(\sum_{q=1}^{Q^b}\Phi_q(\boldsymbol{\mu})\boldsymbol{\sigma}_{qn}\right)\|},$$

$$P_n^{\perp} = I - L_{n-1}L_{n-1}^{\mathrm{T}}, \quad L_i = \{\boldsymbol{\sigma}_1^{\perp}, \ldots, \boldsymbol{\sigma}_i^{\perp}\};$$

(ii) an orthonormalization (GS) on components $\boldsymbol{\sigma}_{qn}$ made off-line ($\boldsymbol{\sigma}_{qn}$ are not depending on $\boldsymbol{\mu}$) to get $\boldsymbol{\sigma}_{qn}^{\perp *}$:

$$\boldsymbol{\sigma}_{qn}^{\perp *} = \frac{P_{qn}^{\perp}\boldsymbol{\sigma}_{qn}}{\|P_{qn}^{\perp}\boldsymbol{\sigma}_{qn}\|},$$

$$P_{qn}^{\perp} = I - L_{q(n-1)}L_{q(n-1)}^{\mathrm{T}}, \quad L_{qi} = \{\boldsymbol{\sigma}_{q1}^{\perp *}, \ldots, \boldsymbol{\sigma}_{qi}^{\perp *}\},$$

Fig. 13 shows the reduction of the condition number of the matrix of the reduced basis linear system by orthonormalizing reduced basis functions (using method (i) for supremizer, including also orthonormalization for velocity and pressure basis functions). A very interesting property (visible also in Fig. 13) is that the condition number is limited and bounded after orthonormalization and not depending on N.

7.2. Approximation stability: other supremizer options

By orthonormalizing the supremizer solutions according to the approach (i) we could lose approximation stability (guaranteed by Lemma 3.1) in the attempt of preserving algebraic stability by reducing the condition number. We can orthonormalize just using method (i) the pressure ξ and the velocity ζ basis functions and not the supremizer σ_n and use the approach (ii) to orthogonalize the supremizer on its component σ_{kn} (before summation) to preserve Lemma 3.1.

To achieve this goal we may introduce two further different options in assembling the supremizer solutions for stabilization procedure by building in a different way the reduced basis velocity approximation space so that we may guarantee both approximation and algebraic stability.

7.2.1. First option

We have considered the following reduced basis spaces:

$$Y_N = \mathrm{span}\{\boldsymbol{\sigma}_n, n = 1, \ldots, N\overline{Q}^b\},$$

where $\overline{Q}^b = Q^b + 1$. For $n = 1, \ldots, N$:

$$\boldsymbol{\sigma}_n = \zeta_n = \mathbf{u}(\boldsymbol{\mu}^n).$$

For $n = N+1, \ldots, N\overline{Q}^b$, condensing index m and k in n, we have $(\boldsymbol{\sigma}_n, \mathbf{w})_Y = (\tilde{\boldsymbol{\sigma}}_{mk}, \mathbf{w})_Y$, where

$$(\tilde{\boldsymbol{\sigma}}_{mk}, \mathbf{w})_Y = \mathscr{B}(\xi_m, \mathbf{w})^k, \quad \forall \mathbf{w} \in Y, \quad k = 1, \ldots, Q^b, \ m = 1, \ldots, N;$$

$$\mathbf{u}_N(\boldsymbol{\mu}) = \sum_{j=1}^{N\overline{Q}^b} u_{Nj}(\boldsymbol{\mu})\boldsymbol{\sigma}_j,$$

$$p_N(\boldsymbol{\mu}) = \sum_{l=1}^{N} p_{Nl}(\boldsymbol{\mu})\xi_l;$$

the reduced basis system becomes

$$\begin{cases} \sum_{j=1}^{N\overline{Q}_b} A_{ij}^{\boldsymbol{\mu}}\mathbf{u}_{Nj}(\boldsymbol{\mu}) + \sum_{l=1}^{N} B_{il}^{\boldsymbol{\mu}}p_{Nl}(\boldsymbol{\mu}) = F_i, \quad 1 \leqslant i \leqslant N\overline{Q}_b, \\ \sum_{j=1}^{N\overline{Q}_b} B_{jl}^{\boldsymbol{\mu}}\mathbf{u}_{Nj}(\boldsymbol{\mu}) = G_l, \quad 1 \leqslant l \leqslant N, \end{cases} \tag{44}$$

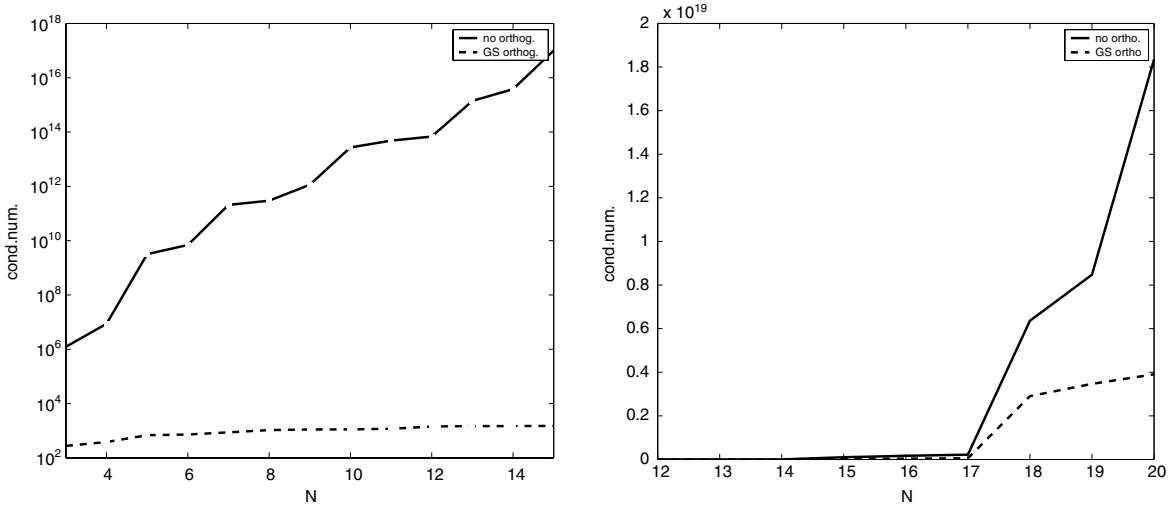

Fig. 13. Orthonormalization: bounded condition number of reduced basis Stokes linear system matrix with complete orthonormalized basis (left) and with a partial orthonormalization only on velocity and pressure (right), but not on supremizer. In each picture there is a comparison with condition number without any orthonormalization.

where

$$A^{\mu}_{ij} = \sum_{k=1}^{Q^a} \Theta^k(\boldsymbol{\mu}) \mathscr{A}(\boldsymbol{\sigma}_i, \boldsymbol{\sigma}_j)^k, \quad 1 \leqslant i, \ j \leqslant N\overline{Q}_b,$$

$$B^{\mu}_{il} = \sum_{k=1}^{Q^b} \Phi^k(\boldsymbol{\mu}) \mathscr{B}(\boldsymbol{\sigma}_i, \xi_l)^k, \quad 1 \leqslant i \leqslant N\overline{Q}_b, \ 1 \leqslant l \leqslant N,$$

$$F_i = \langle F, \boldsymbol{\sigma}_i \rangle, \quad 1 \leqslant i \leqslant N\overline{Q}_b, \ G_l = \langle G^0, \xi_l \rangle, \ 1 \leqslant l \leqslant N.$$

In this case the basis is no longer $\boldsymbol{\mu}$ (on-line) dependent, the reduced basis velocity space, enriched by supremizers, has a bigger dimension ($N\overline{Q}_b > 2N$) than previously. The computational costs are as follows: $O(Q^a(\overline{Q}^b)^2N^2)$ for sub-matrix $\underline{A}$, $O(\overline{Q}^bQ^bN^2)$ for $\underline{B}$, $O(\overline{Q}^bN)$ for $\underline{F}$, but the cost for inversion of the full reduced basis matrix (28) increases now to $O((\overline{Q}^b + 1)^3N^3)$. This approach has the big advantage to preserve Lemma 3.1, to let us apply orthonormalization (method (ii)) and to preserve the mentioned lemma also after orthonormalization. In conclusion this approach is the best if we want to be sure to preserve both algebraic and approximation stability after orthonormalization, if necessary. Fig. 14 shows errors behavior by testing this first new supremizer option over a large test sampling (zero Dirichlet conditions and three geometrical parameters).

7.2.2. Second option

Another approach is based on the idea that supremizers are built upon summation using the same $\boldsymbol{\mu}^j$ values used to store velocity $\zeta_j(\boldsymbol{\mu}^j)$ and pressure solutions $\xi_j(\boldsymbol{\mu}^j)$ (also in this case the basis for velocity is not dependent on the on-line value of $\boldsymbol{\mu}$ and it is completely assembled off-line):

$$Y_N = \text{span}\left\{ \boldsymbol{\sigma}_n = \sum_{k=1}^{\overline{Q}^b} \Phi^k(\boldsymbol{\mu}^n)\boldsymbol{\sigma}_{kn}, \ n = 1, \ldots, 2N \right\},$$

where $\overline{Q}^b = Q^b + 1, \Phi^{\overline{Q}^b} = 1$. For $n = 1, \ldots, N$:

$$\boldsymbol{\sigma}_{kn} = 0, \quad \text{for } k = 1, \ldots, Q^b; \boldsymbol{\sigma}_{\overline{Q}^bn} = \zeta_n = \mathbf{u}(\boldsymbol{\mu}^n).$$

For $n = N+1, \ldots, 2N$:

$$(\boldsymbol{\sigma}_{kn}, \mathbf{w})_Y = \mathscr{B}(\xi_{n-N}, \mathbf{w})^k, \quad \forall \mathbf{w} \in Y, \ \text{for } k = 1, \ldots, Q^b;$$

$$\boldsymbol{\sigma}_{\overline{Q}^bn} = 0.$$

The reduced basis solution is given by

$$\mathbf{u}_N(\boldsymbol{\mu}) = \sum_{j=1}^{2N} u_{Nj}(\boldsymbol{\mu}) \left(\sum_{k=1}^{\overline{Q}^b} \Phi^k(\boldsymbol{\mu}^j)\boldsymbol{\sigma}_{kj} \right),$$

$$p_N(\boldsymbol{\mu}) = \sum_{l=1}^{N} p_{Nl}(\boldsymbol{\mu})\xi_l,$$

by solving the system:

$$\begin{cases} \sum_{j=1}^{2N} A^{\mu}_{ij}\mathbf{u}_{Nj}(\boldsymbol{\mu}) + \sum_{l=1}^{N} B^{\mu}_{il}p_{Nl}(\boldsymbol{\mu}) = F_i, \quad 1 \leqslant i \leqslant 2N, \\ \sum_{j=1}^{2N} B^{\mu}_{jl}\mathbf{u}_{Nj}(\boldsymbol{\mu}) = G_l, \quad 1 \leqslant l \leqslant N, \end{cases} \tag{45}$$

where

$$\begin{aligned} A^{\mu}_{ij} &= \sum_{k=1}^{Q^a} \Theta^k(\boldsymbol{\mu}) \mathscr{A}(\boldsymbol{\sigma}_i, \boldsymbol{\sigma}_j)^k \\ &= \sum_{k=1}^{Q^a} \sum_{k'=1}^{\overline{Q}^b} \sum_{k''=1}^{\overline{Q}^b} \Theta^k(\boldsymbol{\mu}) \Phi^{k'}(\boldsymbol{\mu}^i) \Phi^{k''}(\boldsymbol{\mu}^j) \mathscr{A}(\boldsymbol{\sigma}_{k'i}, \boldsymbol{\sigma}_{k''j})^k, \\ &\qquad 1 \leqslant i, j \leqslant 2N; \end{aligned}$$

$$\begin{aligned} B^{\mu}_{il} &= \sum_{k=1}^{Q^b} \Phi^k(\boldsymbol{\mu}) \mathscr{B}(\boldsymbol{\sigma}_i, \xi_l)^k \\ &= \sum_{k=1}^{Q^b} \sum_{k'=1}^{\overline{Q}^b} \Phi^k(\boldsymbol{\mu}) \Phi^{k'}(\boldsymbol{\mu}^i) \mathscr{B}(\boldsymbol{\sigma}_{k'i}, \xi_l)^k, \\ &\qquad 1 \leqslant i \leqslant 2N, \ 1 \leqslant l \leqslant N; \end{aligned}$$

$$F_i = \langle F, \sigma_i \rangle = \sum_{k'=1}^{\overline{Q}^b} \Phi^{k'}(\boldsymbol{\mu}^i) \langle F, \boldsymbol{\sigma}_{k'i} \rangle, \quad 1 \leqslant i \leqslant 2N,$$

$$G_l = \langle G^0, \xi_l \rangle, \quad 1 \leqslant i, l \leqslant N.$$

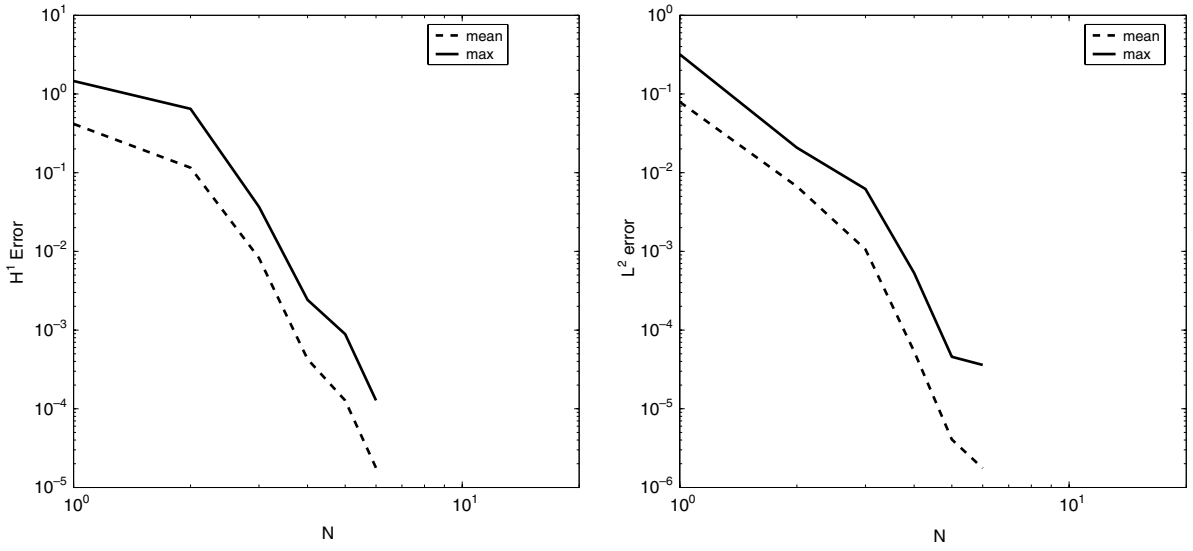

Fig. 14. Supremizer: first option, H^1 relative error (for velocity) and L^2 relative error (for pressure) using 50 configurations.

This option is also competitive as regards the computational costs dealing with $3N \times 3N$ reduced basis matrices (28) instead of $(\overline{Q}^b + 1)N \times (\overline{Q}^b + 1)N$ matrix (usually $(\overline{Q}^b + 1) \gg 3$). We have the following computational costs to build reduced basis matrices, given also the supremizer components in the velocity space: $O(Q^a 4N^2)$ for sub-matrix A, $O(Q^b 2N^2)$ for $\underline{B}$, $O(N)$ for $\underline{F}$ and $O(27N^3)$ for the inversion of the full reduced basis matrix (28).

Using this option we cannot demonstrate that Lemma 3.1 is still valid (even without orthonormalization). We have tested numerically this option and we can argue that also this approximation is reasonably stable. Numerical results are shown in Fig. 15 where we have reported errors behavior always testing a large number of configurations (Dirichlet conditions and three varying parameters as in Section 6.3). Convergence is very fast in this case. Fig. 16 shows the condition number reduction of reduced basis linear system and a comparison of condition number of the matrix without orthonormalization.

8. Perspectives

Development guidelines are devoted to the application of reduced basis to Navier–Stokes equations in parametrized domains and in problems involving non-affine mapping dependence (i.e., shape design problem). See [31] for Navier–Stokes reduced basis formulation and [30,2] for non-affine parametric dependence in elliptic problems. The latter reference especially introduces an efficient reduced basis discretization procedure replacing non-affine coefficient functions with a collateral reduced basis expansion which permits an off-line/on-line computational decomposition by a stable and inexpensive interpolation procedure. This approach allows us the introduction of curved elements in parametrized geometries. The interest is to expand and apply efficient, accurate and real-time reduced basis techniques on bio-mechanics problems (i.e., bio-medical devices optimization such as bypass [21,26,27]). The most important steps under investigation

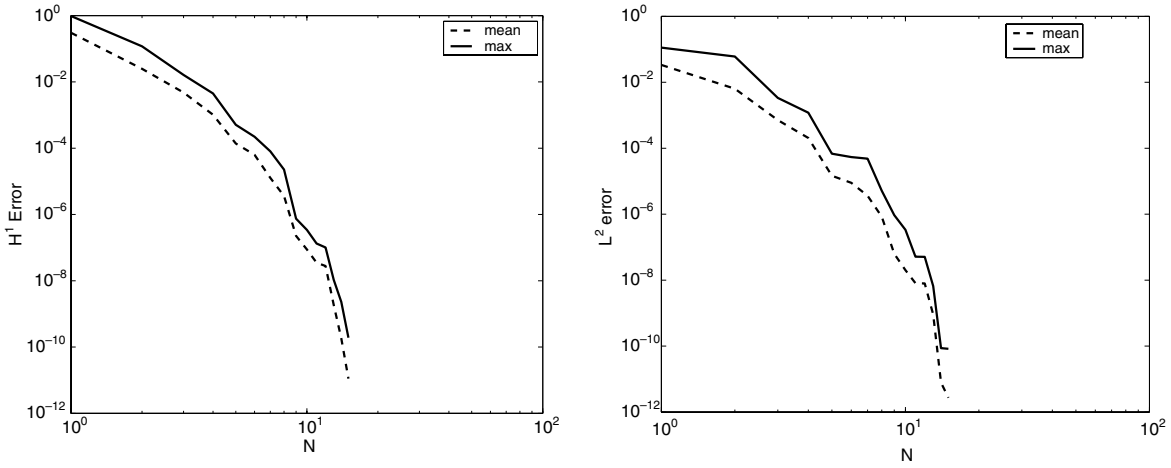

Fig. 15. Supremizer: second option, H^1 relative error (velocity) and L^2 relative error (pressure) over 50 configurations.

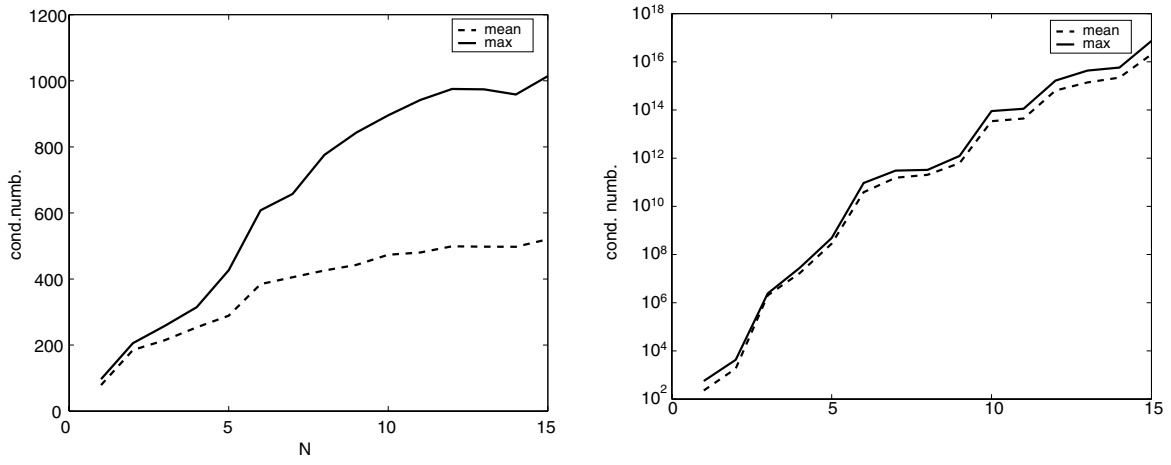

Fig. 16. Condition number (max and mean) for the Stokes reduced basis system, with the new supremizer second option. On the left results with orthonormalization, on the right without it.

are (i) the use of a great number of geometrical parameters, (ii) the non-affine formulation for Stokes reduced basis problem ([28]) and (iii) the study of a posteriori error bounds for Stokes equations.

Acknowledgements

We acknowledge Prof. A.T. Patera of MIT, Prof. A. Quarteroni of EPF-Lausanne and MOX-Politecnico di Milano and Prof. Y. Maday of University Paris VI, Dr. D. Rovas (University of Illinois), Dr. C. Prud'homme (EPFL) and Dr. N.C. Nguyen (National University of Singapore) for suggestions, very helpful discussion, comments and insights, Prof. F. Saleri (MOX-Politecnico di Milano) for providing the original finite element Stokes solver. G. Rozza acknowledges the support provided through the European Community's Human Potential Programme under contract HPRN-CT-2002-00270 HaeMOdel. This work was supported also by Swiss National Science Foundation (PBEL2-111646), by DARPA and ASFOR under grant F4920-03-1-0356, by DARPA and GEAE under grant F49620-03-1-0439 and by Singapore–MIT Alliance (SMA).

References

[1] E. Balmes, Parametric families of reduced finite element models: theory and applications, Mech. Syst. Signal Process. 10 (4) (1996) 381–394.
[2] M. Barrault, Y. Maday, N.C. Nguyen, A.T. Patera, An "empirical interpolation" method: application to efficient reduced-basis discretization of partial differential equations, C.R. Acad. Sci. Paris, Ser. I 339 (2004) 667–672.
[3] A. Barrett, G. Reddien, On the reduced basis method, Z. Angew. Math. Mech. 75 (7) (1995) 543–549.
[4] J.P. Fink, W.C. Rheinboldt, On the error behavior of the reduced basis technique for nonlinear finite element approximations, Z. Angew. Math. Mech. 63 (1) (1983) 21–28.
[5] G.P. Galdi, An introduction to the mathematical theory of the Navier–Stokes equations, Linearized Steady Problem, vol. I, Springer-Verlag, New York, 1994.
[6] V. Girault, P.A. Raviart, Finite Element Methods for Navier–Stokes Equations, Springer-Verlag, Berlin, 1986.
[7] P.M. Gresho, R.L. Sani, Incompressible Flow and the Finite Elements Method, Wiley, New York, 2000.
[8] M.D. Gunzburger, Finite Element Method for Viscous Incompressible Flows: A Guide to Theory, Practice, and Algorithms, Academic Press, Boston, 1989.
[9] K. Ito, S.S. Ravindran, A reduced basis method for control problems governed by PDEs, in: W. Desch, F. Kappel, K. Kunish (Eds.), Control and Estimation of Distributed Parameter System, Birka·user, Basel, 1998, pp. 153–168.
[10] K. Ito, S.S. Ravindran, A reduced-order method for simulation and control of fluid flow, J. Comput. Phys. 143 (2) (1998) 403–425.
[11] Y. Maday, A.T. Patera, G. Turinici, Global a priori convergence theory for reduced-basis approximations of single-parameter symmetric coercive elliptic partial differential equations, C.R. Acad. Sci. Paris, Sér. I 335 (2002) 1–6.
[12] Y. Maday, A.T. Patera, G. Turinici, A priori convergence theory for reduced-basis approximations of single-parameter elliptic partial differential equations, J. Sci. Comput. 17 (1) (2002) 437–446.
[13] D.S. Malkus, Eigenproblems associated with the discrete LBB condition for incompressible finite elements, Int. J. Engrg. Sci. 19 (1981) 1299–1310.
[14] N.C. Nguyen, K. Veroy, A.T. Patera, Certified real-time solution of parametrized partial differential equations, in: R. Catlow, H. Shercliff, S. Yip (Eds.), Handbook of Materials Modeling, Kluwer Academic Publishing (Springer), Dordrecht, 2005.
[15] J.S. Peterson, The reduced basis method for incompressible viscous flow calculations, SIAM J. Sci. Stat. Comput. 10 (4) (1989) 777–786.
[16] T.A. Porsching, Estimation of the error in the reduced basis method solution of nonlinear equations, Math. Comput. 45 (172) (1985) 487–496.
[17] C. Prud'homme, Adaptive reduced basis space generation and approximation, submitted for publication.
[18] C. Prud'homme, D. Rovas, K. Veroy, Y. Maday, A.T. Patera, G. Turinici, Reliable real-time solution of parametrized partial differential equations: reduced-basis output bound methods, J. Fluids Engrg. 172 (2002) 70–80.
[19] C. Prud'homme, A.T. Patera, Reduced-basis output bounds for approximately parametrized elliptic coercive partial differential equations, Comput. Visual. Sci. 6 (2–3) (2004) 147–162.
[20] C. Prud'homme, D. Rovas, K. Veroy, A.T. Patera, Mathematical and computational framework for reliable real-time solution of parametrized partial differential equations, M2AN 36 (5) (2002) 747–771.
[21] A. Quarteroni, G. Rozza, Optimal control and shape optimization of aorto-coronaric bypass anastomoses, M^3AS 13 (12) (2003) 1801–1823.
[22] A. Quarteroni, R. Sacco, F. Saleri, Numerical Mathematics, Springer, New York, 2000.
[23] A. Quarteroni, A. Valli, Numerical Approximation of Partial Differential Equations, Springer-Verlag, Berlin, 1994.
[24] W.C. Rheinboldt, On the theory and error estimation of the reduced basis method for multi-parameter problems, Nonlin. Anal. Theory, Methods Appl. 21 (11) (1993) 849–858.
[25] D. Rovas, Reduced-basis output bound methods for parametrized partial differential equations, PhD Thesis, MIT – Massachusetts Institute of Technology, February 2003.
[26] G. Rozza, On optimization, control and shape design of an arterial bypass, Int. J. Numer. Methods Fluids 47 (10–11) (2005) 1411–1419.
[27] G. Rozza, Real time reduced basis techniques for arterial bypass geometries, in: K.J. Bathe (Ed.), Computational Fluid and Solid Mechanics, Elsevier, Amsterdam, 2005, pp. 1283–1287.
[28] G. Rozza, Reduced basis methods for Stokes equations in domains with non-affine parameter dependence, EPFL-IACS report 06.2005, Comput. Visual. Sci., submitted for publication.
[29] G. Rozza, Shape design by optimal flow control and reduced basis techniques: applications to bypass configurations in haemodynamics, PhD Thesis No. 3400, EPFL, Ecole Polytechnique Fédérale de Lausanne, 2005.
[30] Y. Solodukhov, Reduced-basis methods applied to locally non-affine problems, PhD thesis, MIT, Massachusetts Institute of Technology, 2004.
[31] K. Veroy, A.T. Patera, Certified real-time solution of the parametrized steady incompressible Navier–Stokes equations: rigorous reduced-basis a posteriori error bounds, Int. J. Numer. Methods Fluids 47 (8–9) (2005) 773–788.
[32] K. Veroy, A.T. Patera, Reduced-basis approximation of the viscosity-parametrized incompressible Navier–Stokes equations: rigorous a posteriori error bounds, in: Proceedings Singapore–MIT Alliance Symposium, January 2004.
[33] K. Veroy, Reduced-basis methods applied to problems in elasticity, PhD Thesis, MIT – Massachusetts Institute of Technology, June 2003.
[34] K. Veroy, C. Prud'homme, D. Rovas, A.T. Patera, A posteriori error bounds for reduced-basis approximation of parametrized noncoercive and nonlinear elliptic partial differential equations, AIAA American Institute of Aeronautics and Astronautics, Paper 2003–3847, 2003.